TNO report
FEL-96-B216

Design of the PHARUS radome; Electrical aspects

TNO Physics and Electronics Laboratory

Oude Waalsdorperweg 63
PO Box 96864
2509 JG The Hague
The Netherlands

Phone +31 70 374 00 00
Fax +31 70 328 09 61

Date
November 1996

Author(s)
M.H.A. Paquay

Classification		
Classified by	:	H.R. van Es
Classification date	:	October 1996
Title	:	Ongerubriceerd
Managementuittreksel	:	Ongerubriceerd
Abstract	:	Ongerubriceerd
Report text	:	Ongerubriceerd
Appendix A	:	Ongerubriceerd

Copy no	:	8	
No of copies	:	28	
No of pages	:	45	(incl appendix, excl RDP & distribution list)
No of appendices	:	1	

All information which is classified according to Dutch regulations shall be treated by the recipient in the same way as classified information of corresponding value in his own country. No part of this information will be disclosed to any party.

The classification designation Ongerubriceerd is equivalent to Unclassified, Stg. Confidentieel is equivalent to Confidential and Stg. Geheim is equivalent to Secret.

The TNO Physics and Electronics Laboratory is part of TNO Defence Research which further consists of:

TNO Prins Maurits Laboratory
TNO Human Factors Research Institute

Netherlands Organization for Applied Scientific Research (TNO)

Managementuittreksel

Titel	:	Design of the PHARUS radome; Electrical aspects
Auteur(s)	:	Ir. M.H.A. Paquay
Datum	:	november 1996
Opdrachtnr.	:	-
IWP-nr.	:	767.3
Rapportnr.	:	FEL-96-B216

Een radome is een RF-transparant venster of lens voor een antenne. De functie van een radome is de antenne te beschermen tegen invloeden van de omgeving, zoals vocht, (zure) regen, deeltjes etc. Voor een vliegend radarsysteem, zoals PHARUS, is een dergelijke bescherming pure noodzaak.

Tegenwoordig zijn supervezels erg populair bij radome-ontwerpers, omdat deze vezels een goed compromis vormen tussen mechanische sterkte en doorlaatbaarheid voor radiogolven. De PHARUS-radome is gebaseerd op een Dyneema®-composiet. Dit is een samenstelling van een polyethyleen vezel en een polyethyleen film. Onder druk en hoge temperatuur verhardt dit materiaal.

Iedere diëlektirsche laag, dus ook een radome, kan kruispolarisatie tot gevolg hebben, omdat de polarisatiecomponenten van de invallende golf, te scheiden in een componentenparallel en loodrecht op het vlak van inval, een andere transmissiekarakteristiek hebben. Daarnaast is een radome ook een discontinuïteit in de transmissieweg, met als gevolg dat een gedeelte van de invallende golf gereflecteerd wordt. Dit worden de reflectieverliezen genoemd.

Om tot een radome-ontwerp te komen dat zo goed mogelijk zou voldoen aan alle randvoorwaarden, zijn simulaties uitgevoerd. Deze simulaties zijn gebaseerd op een combinatie van de Single Ray Tracing methode en de Transmission Line Equivalence methode.
Uit deze simulaties is naar voren gekomen dat de kruispolaire zuiverheid voornamelijk bepaald wordt door de vorm van de radome. De reflectieverliezen zijn afhankelijk van de dikte van de radome. Met inachtneming van de mechanische beperkingen met betrekking tot gewicht en maximale afmetingen is gebleken dat een radome met een straal van 207,5 mm en een dikte van 4 mm het best bereikbare compromis is.

Metingen aan de uiteindelijk gerealiseerde PHARUS-radome laten zien dat de kruispolarisatie van de antenne niet verslechtert door de radome.

De analysemethode is bruikbaar en betrouwbaar gebleken en de gerealiseerde radome voldoet aan alle gestelde eisen.

® Dyneema is a registered trademark of DSM, Netherlands

Contents

1. Introduction

A radome is an RF transparent window or lens in front of the antenna. Its purpose is to protect the antenna against harsh environmental conditions like moisture, (acid) rain, particles etc. An airborne system like PHARUS cannot do without a protective radome.

PHARUS is an airborne full-polarimetric C-band SAR system for Remote Sensing applications. The antenna is a phased array, consisting of printed microstrip patch radiators. More information about PHARUS can be found in [1].

Nowadays, high performance fibres are very popular for radome design since they allow a good compromise between mechanical strength and RF-transparency. The PHARUS radome is based on a Dyneema®-composite. This is a polyethylene fibre embedded in a polyethylene adhesive. The material is hardened under pressure (20 bar) and high temperature.

However, a radome, like any other dielectric layer, can cause additional cross-polarisation since the polarisation components parallel and perpendicular to the plane of incidence have different transmission characteristics. Besides that, the radome is also a discontinuity in the propagation path, so it will reflect a part of the incident field. This is called the reflection loss.

To cope with all the aspects in the design of the radome, some simulations have been made. This report describes the analysis method and shows some results of the simulations. The reader is assumed to be familiar with the fundamentals of Electro-Magnetic Theory.

® Dyneema is a registered trademark of DSM, Netherlands

2. Reflections and transmissions

Most radomes consist of one or more homogeneous dielectric layers. This chapter describes the analysis method for the reflection and transmission characteristics based on the dielectric constants of the layers.

Many analysis methods are described in literature, ranging from Moment Methods and full surface integrals to ray tracing methods. The method used here is a combination of a single-ray tracing technique and transmission line analysis. It is an approximation, but it represents a good balance between accuracy and computational power. The description of Hirsch and Grove [2] served as a guideline.

For the fundamentals of reflection and transmission of electromagnetic waves at a boundary of 2 dielectric layers, the reader is referred to common literature on Electro-Magnetic Theory.

2.1 Interactions at a boundary

As an electro-magnetic wave encounters a change of medium, part of the wave is reflected into the same medium and another part is transmitted into the other medium. Solving the Maxwell's equations for such a boundary yields some continuity relationships for the electromagnetic fields. These continuity relationships for electric and magnetic fields at a boundary without surface charge are:

- The tangential components of the Electric fields ($\bar{E}$) and Magnetic fields ($\bar{H}$) are continuous, that is equal on both sides of the boundary.
- The normal components of the Electric flux density ($\bar{D}$) and the Magnetic flux density ($\bar{B}$) are continuous.

Figure 2.1 shows the interaction of an electromagnetic field with a boundary between two dielectric layers.

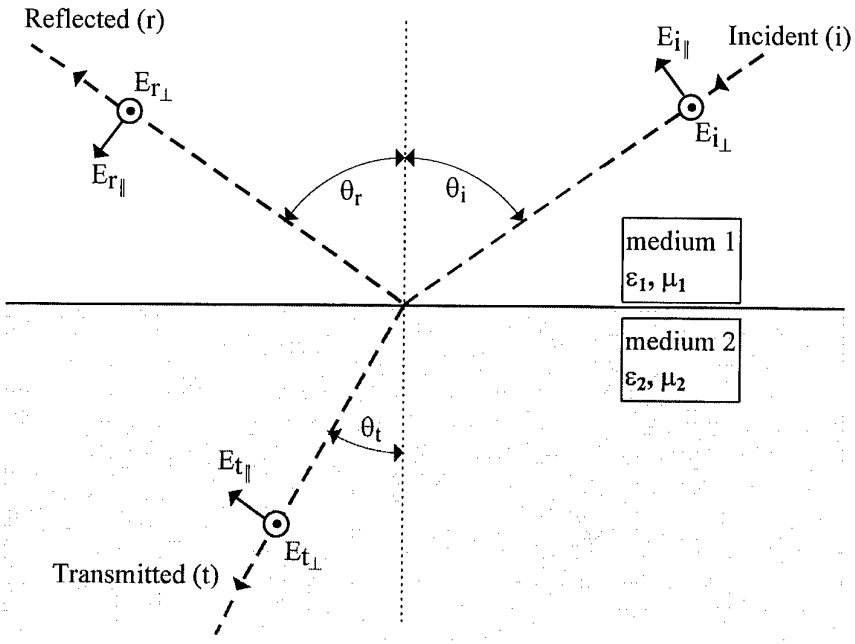

Figure 2.1: Interaction at the boundary of two media

In figure 2.1, the page is called the incidence plane which is defined by a vector normal to the boundary and the propagation vector of the incident field.

The interaction is described by means of an incident field, a reflected field and a transmitted field. The continuity relationships give rise to decompose the field in components parallel ($\parallel$) or perpendicular ($\perp$) to the plane of incidence. In figure 2.1, only the electric field components are shown. The corresponding magnetic field vectors are chosen in such a way that the Poynting vector $\vec{S}\,(=\vec{E}\times\vec{H})$ is in the direction of propagation.

Solving the continuity relationships yields the following results:

- The angle of reflection is equal to the angle of incidence
- The angle of transmission is related to the angle of incidence by Snell's law:

$$\sin(\theta_t) = \sqrt{\mu_1\varepsilon_1/\mu_2\varepsilon_2}\,\sin(\theta_i) \tag{2.1}$$

The reflection coefficients of the parallel and perpendicular electric components are given by:

$$\rho_{\parallel} = \frac{E_{r\parallel}}{E_{i\parallel}} = \frac{Z_2\cos(\theta_t) - Z_1\cos(\theta_i)}{Z_1\cos(\theta_i) + Z_2\cos(\theta_t)} \tag{2.2}$$

$$\rho_{\perp} = \frac{E_{r\perp}}{E_{i\perp}} = \frac{Z_2 \cos(\theta_i) - Z_1 \cos(\theta_t)}{Z_2 \cos(\theta_i) + Z_1 \cos(\theta_t)} \tag{2.3}$$

in which the characteristic impedance (sometimes called intrinsic impedance) of layer n is given by:

$$Z_n = \sqrt{\mu_n / \varepsilon_n} \qquad \begin{array}{l} \mu_n = \text{permeability of layer n} \\ e_n = \text{permittivity of layer n} \end{array} \tag{2.4}$$

The transmission coefficients are given by

$$\tau_{\parallel} = \frac{E_{t\parallel}}{E_{i\parallel}} = (\rho_{\parallel} + 1)\frac{\cos(\theta_i)}{\cos(\theta_t)} \tag{2.5}$$

$$\tau_{\perp} = \frac{E_{t\perp}}{E_{i\perp}} = (\rho_{\perp} + 1) \tag{2.6}$$

These equations can be used to describe the reflection and transmission characteristics of dielectric layers.

2.2 Transmission Line Equivalent

The simplest radome is a single layer as shown in figure 2.2.

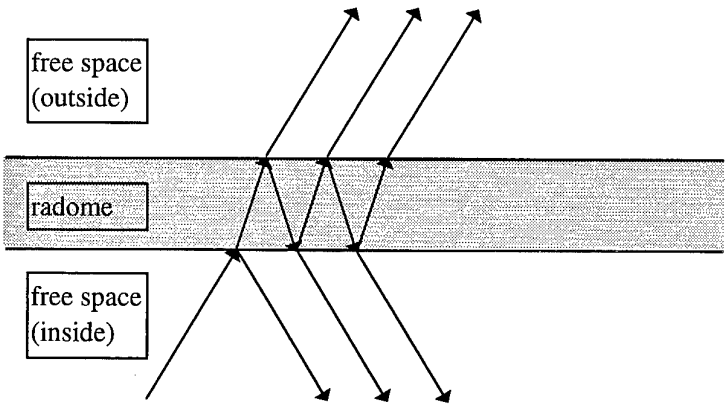

Figure 2.2: Reflection and transmission through a radome

Let's call the region below the radome the inside part and the region above the radome the outside part.

A wave coming from the inside will be reflected partly and the remaining is transmitted into the radome. The transmitted part will interact with the outside of the radome. Again, some part will be transmitted to the outside region and the rest is reflected back into the radome. This process repeats every time the wave reaches the inside or outside of the radome. The total transmission or reflection characteristics can be described as an infinite summation over all the single and multiple bounced contributions. Another way is to look for the steady state solution.

There is an equivalent problem with transmission lines. Figure 2.3 shows two pieces of transmission line, terminated with a load impedance.

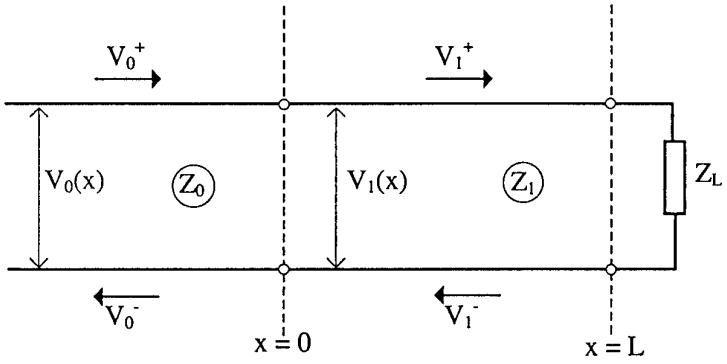

Figure 2.3: Signals on a Transmission Line

Every interaction of the signal with discontinuities at x = 0 and x = L will cause reflections and transmissions. On all parts of the transmission line of figure 2.3, signals are propagating to the left and to the right. On line part 0, the signal travelling to the right has amplitude V_0^+. The signal travelling to the left has amplitude V_0^-. The amplitude of the signal at any place on part 0 is:

$$V_0(x) = V_0^+ \exp(-\gamma_0 x) + V_0^- \exp(\gamma_0 x) \tag{2.7}$$

where $\gamma = \alpha + j\beta$

$\beta = 2\pi/\lambda$

Similar for part 1:

$$V_1(x) = V_1^+ \exp(-\gamma_1 x) + V_1^- \exp(\gamma_1 x) \tag{2.8}$$

The reflection at the load impedance at x = L is described as:

$$\rho_L = \frac{V_1^- \exp(\gamma_1 L)}{V_1^+ \exp(-\gamma_1 L)} = \frac{Z_L - Z_1}{Z_L + Z_1} \tag{2.9}$$

The interactions at x = 0 are described as:

$$V_1^+ = \rho_{10} V_1^- + \tau_{01} V_0^+ \tag{2.10a}$$

$$V_0^- = \rho_{01} V_0^+ + \tau_{10} V_1^- \tag{2.10b}$$

where ρ_{10} is the reflection coefficient for signals coming from part 1 at the boundary with part 0. τ_{10} is the transmission coefficient from part 1 to part 0. Their relations to the characteristic impedances are:

$$\rho_{10} = \frac{Z_0 - Z_1}{Z_0 + Z_1} \tag{2.11a}$$

$$\tau_{10} = 1 + \rho_{10} \tag{2.11b}$$

$$\rho_{01} = \frac{Z_1 - Z_0}{Z_1 + Z_0} = -\rho_{10} \tag{2.11c}$$

$$\tau_{01} = 1 + \rho_{01} \tag{2.11d}$$

The relations (2.11b) and (2.11d) look counterintuitive, however they follow directly from the continuity relationship at x = 0:

$$V_0(x = 0) = V_1(x = 0) \Leftrightarrow V_0^+ + V_0^- = V_1^+ + V_1^- \tag{2.12}$$

Assuming that $V_0^+ = 0$ or $V_1^+ = 0$ and using the relations of (2.10) (2.12), yields (2.11b) or (2.11d). In the electromagnetic case, similar relationships can be derived from the continuity relationship of the electric field ($E_r + E_i = E_t$).

Requested is the total reflection of the incident signal V_0^+ at x = 0:

$$\rho_{tot} = \frac{V_0^-}{V_0^+} \tag{2.13}$$

and the total transmission from the incident signal to the load:

$$\tau_{L0} = \frac{V_L}{V_0^+} \tag{2.14}$$

Solving the system of equations (2.7) - (2.11) yields

$$\rho_{tot} = \rho_{01} + \frac{\rho_L (1 + \rho_{01}\rho_{10}) \exp(-2\gamma_1 L)}{1 - \rho_L \rho_{10} \exp(-2\gamma_1 L)} \tag{2.15}$$

$$\tau_{L0} = \frac{\tau_{01}(1+\rho_L)\exp(-\gamma_1 L)}{1-\rho_{10}\rho_L \exp(-2\gamma_1 L)} \tag{2.16}$$

Another approach is to calculate the impedance transformation by transmission line part 1:

$$\frac{Z(x)}{Z_1} = \frac{1+\rho(x)}{1-\rho(x)} \tag{2.17}$$

$$\rho(x) = \frac{V_1^-(x)}{V_1^+(x)} = \frac{V_1^- \exp(\gamma_1 x)}{V_1^+ \exp(-\gamma_1 x)} = \frac{V_1^-}{V_1^+}\exp(2\gamma_1 x) \tag{2.18}$$

$$\Rightarrow \quad \rho(0) = \rho(L)\exp(-2\gamma_1 L) \tag{2.19}$$

For convenience, the following notation will be used:

$Z_L = Z(x = L)$

$$\rho_L = \rho(x = L) = \frac{Z_L - Z_1}{Z_L + Z_1}$$

Z(0) is the impedance at x = 0 as seen by the transmission line part 0.

$$Z(0) = Z_1 \frac{1+\rho(0)}{1-\rho(0)} = Z_1 \frac{1+\rho_L \exp(-2\gamma_1 L)}{1-\rho_L \exp(-2\gamma_1 L)} \tag{2.20}$$

$$\rho_{tot} = \frac{Z(0) - Z_0}{Z(0) + Z_0} \tag{2.21}$$

By straightforward analysis it can be shown that substituting (2.20) in (2.21) yields the same result as (2.15).

The method can be expanded to multiple discontinuities, resulting in multiple parts of the transmission line. The load impedance is transformed to an equivalent impedance at the previous discontinuity. This process is repeated till the equivalent impedance at the first discontinuity is known. Then, in the reverse direction, the propagation can be solved for the successive parts which finally yields the total transmission from input to load impedance.

The equivalence with the propagation through a radome is clear. The load impedance is the free space impedance of the outer space (377 Ω). It is a pure resistive impedance because of the assumption that the radiated energy disappears in the free space. The path length through a layer is dependant on the thickness of the layer and the angle of transmission.

3. Radome analysis

The radome analysis follows the path of a single ray through the radome. At each transition, the reflection and transmission characteristics are determined. Using the method as described in the previous chapter, the reflection and transmission characteristics for the whole radome are determined. The steps in the analysis are:

1. Calculate the point of intersect and determine the angle of incidence
2. Calculate the angles of incidence on all layer transitions, using single-ray tracing from inside to outside.
3. Decompose the incidence electric field in parallel and perpendicular components
4. Calculate the total transmission and reflection coefficients for both the parallel and perpendicular polarisation by calculating the equivalent impedances at the layer transitions, from outside to inside.
5. Compose the transmitted and reflected fields from their parallel and perpendicular components.
6. Calculate depolarisation effects, reflection loss, phase shift etc. by comparing the transmitted or reflected field to the incident field.

It might be clear from this scheme that the geometry of the radome plays an important role in the calculation. The shape depends very much on the radar system. To use the described method, the geometry calculations have to be adapted for every new design. Besides that, only a limited number of well defined mathematical shapes will be practical for this method. On the other hand, for those cases it is a simple and fast method with reasonable accuracy which allows interactive designing or even CAD.

3.1 PHARUS radome geometry

The PHARUS array antenna consists of 2 x 24 elements. It is prepared for expansion to 4 x 24 elements. This long and narrow configuration can be approximated by a line radiator. The ideal shape is half a cylinder with the radiator in its centre. Unfortunately, the diameter of the whole system is restricted to avoid contact with the ground during take-off and landing. (The radar is mounted at the outside of the aircraft). Furthermore, the framewidth (350 mm) and the position of the antenna in relation to the frame (16.6 mm behind the frame aperture) were defined. So the remaining design parameters are the height of the radome above the frame (max. 100 mm) and the thickness of the radome. Fig. 3.1 shows the configuration.

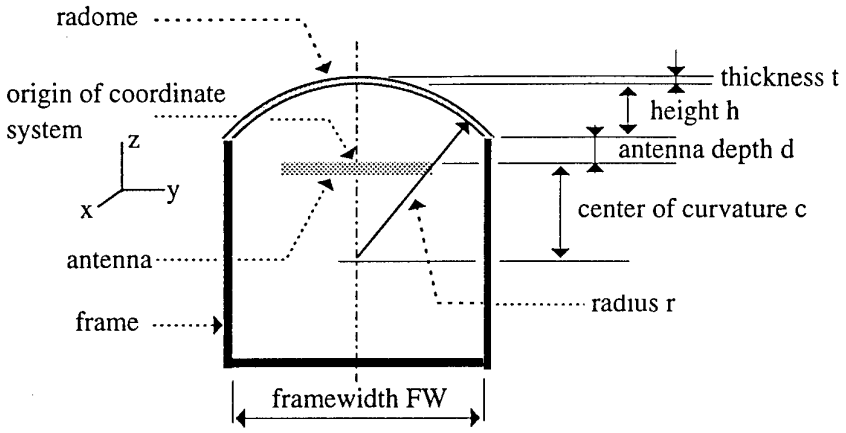

Figure 3.1: PHARUS radome geometry

The inside radius of the radome is determined by the height and the framewidth. From the relations

$$r = c + d + h \tag{3.1}$$

and

$$r^2 = (c + d)^2 + (FW / 2)^2 \tag{3.2}$$

there can be derived

$$r = \frac{FW^2}{8h} + \frac{h}{2} \tag{3.3}$$

The mathematical description of the radome is

$$y^2 + (z + c)^2 = r^2 \tag{3.4}$$

3.2 Point of intersect

For the ray tracing it is assumed that the ray starts in the origin and the direction of propagation is given by an azimuth and elevation angle. In this case, where the antenna is in the X-Y-plane, azimuth is defined as the angle between the Z-axis and the projection of the propagation vector on the XZ-plane (see fig. 3.2). Elevation is the angle between the propagation vector and its projection on the XZ-plane.

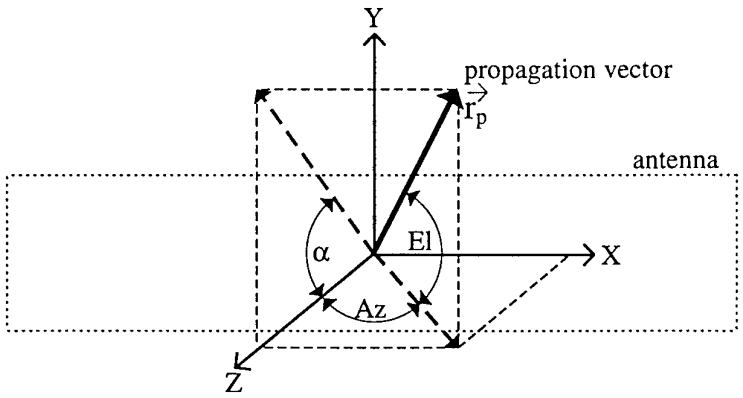

Figure 3.2: Propagation vector in Azimuth-Elevation co-ordinate system

Following this definition, the propagation vector $\vec{r}_P$ is described as:

$$\begin{aligned}\vec{r}_P &= P\cos(El).\sin(Az)\vec{e}_X + P\sin(El)\vec{e}_Y + P\cos(El).\cos(Az)\vec{e}_Z \\ &= x_P\vec{e}_X + y_P\vec{e}_Y + z_P\vec{e}_Z\end{aligned} \tag{3.5}$$

($\vec{e}_X$, $\vec{e}_Y$ and $\vec{e}_Z$ are unit vectors in respectively the x, y and z - direction)

As help, it is useful to define the angle between the projection of $\vec{r}_P$ on the YZ-plane and the Z-axis as α. The relation between α and the azimuth and elevation is

$$\tan(\alpha) = \frac{y_P}{z_P} = \frac{\tan(El)}{\cos(Az)} \tag{3.6}$$

The projection of $\vec{r}_P$ on the YZ-plane can now be written as

$$\vec{r}_{Pyz} = P'\sin(\alpha)\vec{e}_Y + P'\cos(\alpha)\vec{e}_Z \tag{3.7}$$

The intersection of this vector $\vec{r}_{Pyz}$ with the radome can be determined by substituting (3.7) in (3.4), yielding

$$P' = -c.\cos(\alpha) + \sqrt{r^2 - c^2\sin^2(\alpha)} \tag{3.8}$$

The y_P and z_P can be calculated by substituting (3.8) in (3.7). The x_P-component can be calculated by

$$x_P = z_P.\tan(Az) \tag{3.9}$$

Conclusion: the co-ordinates of the point of intersect are

$$\vec{r}_P = (P'.\cos(\alpha).\tan(Az), P'.\sin(\alpha), P'.\cos(\alpha)) \tag{3.10}$$

3.3 Angle of Incidence

The angle of incidence can be calculated using the inner product (also called dot product) of the propagation vector and the vector normal to the radome surface (see figure 3.3).

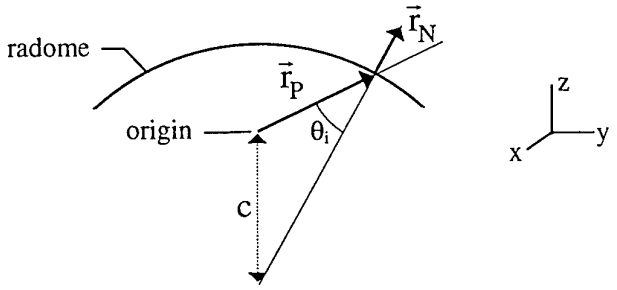

Figure 3.3: Angle of incidence

$$(\vec{r}_P \bullet \vec{r}_N) = |\vec{r}_P| \cdot |\vec{r}_N| \cdot \cos(\theta_i) = |\vec{r}_P| \cdot \cos(\theta_i) \tag{3.11}$$

(By definition, the length of a normal vector is equal to 1)

$$\vec{r}_N = \frac{y_P \vec{e}_Y + (z_P + c)\vec{e}_Z}{\sqrt{y_P^2 + (z_P + c)^2}} \tag{3.12}$$

The normalised version of the propagation vector $\vec{r}_P / |\vec{r}_P|$ is also called the look vector $\vec{r}_L$.

3.4 Angle of transmission and path length

The angle of transmission can be calculated using Snell's law (2.1).
The path length through the first layer of the radome is (see also figure 3.4):

$$l_1 = h_1 / \cos(\theta_t) \tag{3.13}$$

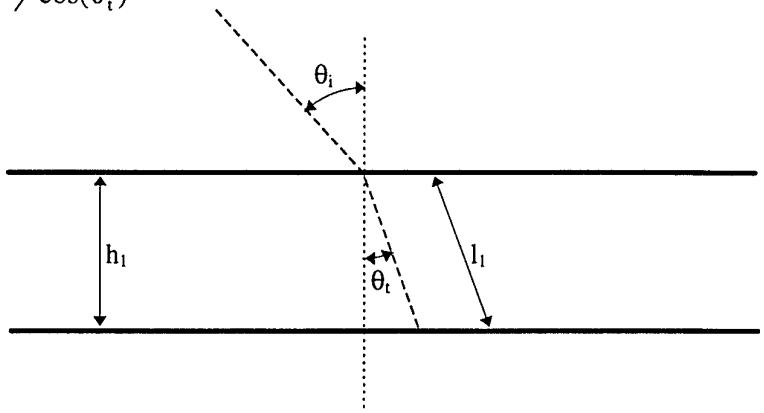

Figure 3.4: path length through layer 1

In the case of a multilayer radome, the calculated angle of transmission is equal to the angle of incidence of the next boundary under the assumption that the radome can be treated as a local planar structure. From Snell's law, the angle of transmission in the next layer can be calculated. These steps have to be repeated through the whole radome. The final angle of transmission of a planar structure is equal to the original angle of incidence, as can be proven as follows:

Assume the radome has n layers. Boundary m is the transition from layer m to m+1. The angle of transmission of boundary m is the angle of incident at boundary m+1:

$$\theta_{i_{m+1}} = \theta_{t_m} \tag{3.14}$$

The final angle of transmission θ_{t_n} can be derived from

$$\begin{aligned} \sin(\theta_{t_n}) &= \sqrt{\varepsilon_n/\varepsilon_{n+1}}\,\sin(\theta_{i_n}) = \sqrt{\varepsilon_n/\varepsilon_{n+1}}\,\sin(\theta_{t_{n-1}}) \\ &= \left(\prod_{m=0}^{n}\sqrt{\frac{\varepsilon_m}{\varepsilon_{m+1}}}\right)\sin(\theta_{i_0}) = \frac{\varepsilon_0\prod_{m=1}^{n}\sqrt{\varepsilon_m}}{\varepsilon_{n+1}\prod_{m=0}^{n-1}\sqrt{\varepsilon_{m+1}}}\sin(\theta_{i_0}) \\ &= \frac{\varepsilon_0}{\varepsilon_{n+1}}\sin(\theta_{i_0}) = \sin(\theta_{i_0}) \end{aligned} \tag{3.15}$$

3.5 Decomposition of electric fields

PHARUS is a full polarimetric radar system. In the transmit mode it can radiate either horizontal or vertical polarisation, in the receive mode it receives both polarisations simultaneously.

On the antenna aperture, that is the XY-plane of figure 3.2, the horizontal polarisation is directed along the X-axis, the vertical polarisation is along the Y-axis. Following the commonly used third definition of Ludwig [3] the vertical and horizontal polarisation are given by

$$\begin{aligned}\vec{e}_V = &\left[(\cos(\theta)-1).\sin(\varphi).\cos(\varphi)\right]\vec{e}_X + \\ &\left[1+(\cos(\theta)-1).\sin^2(\varphi)\right]\vec{e}_Y + \\ &\left[-\sin(\theta).\sin(\varphi)\right]\vec{e}_Z\end{aligned} \tag{3.16a}$$

$$\begin{aligned}\vec{e}_H = &\left[1+(\cos(\theta)-1).\cos^2(\varphi)\right]\vec{e}_X + \\ &\left[\sin(\varphi).\cos(\varphi).(\cos(\theta)-1)\right]\vec{e}_Y + \\ &\left[-\sin(\theta).\cos(\varphi)\right]\vec{e}_Z\end{aligned} \tag{3.16b}$$

Figure 3.5 shows the relation between the Azimuth-Elevation co-ordinates and the spherical co-ordinates.

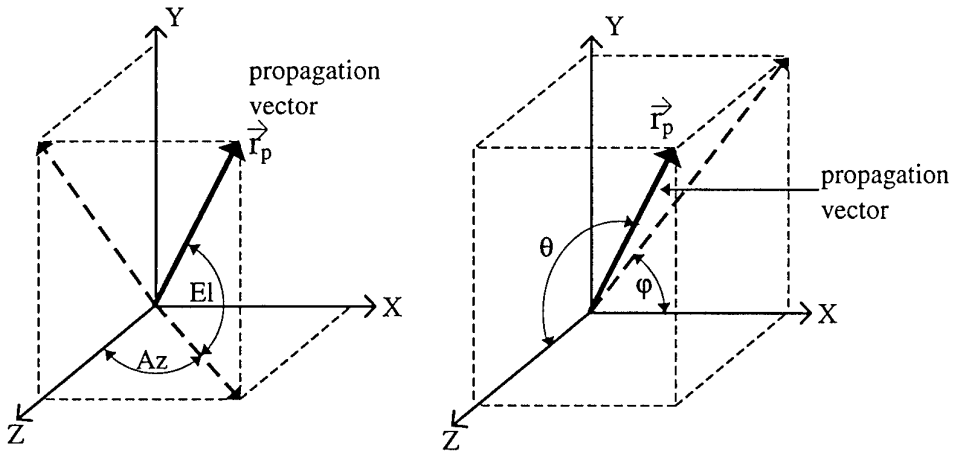

Figure 3.5: Azimuth-Elevation co-ordinates (left) and spherical co-ordinates (right).

The following relations can be used to translate the co-ordinates:

$$\begin{aligned}\tan(Az) &= \tan(\theta).\cos(\varphi) & \tan(\varphi) &= \tan(El)/\sin(Az) \\ \sin(El) &= \sin(\theta).\sin(\varphi) & \cos(\theta) &= \cos(El).\cos(Az)\end{aligned} \tag{3.17}$$

The horizontal and vertical vector have to get decomposed in components parallel and perpendicular to the plane of incidence (see fig. 2.1). The perpendicular vector is perpendicular to the (normalised) vector normal to the radome surface and the propagation or (normalised) look vector. The perpendicular unit vector at the incident point can be defined as the outer product of the look vector $\vec{r}_L$ and the surface normal vector $\vec{r}_N$:

$$\vec{r}_\perp = \vec{r}_L \times \vec{r}_N \tag{3.18}$$

The parallel unit vector is perpendicular to the perpendicular unit vector and the surface normal vector, so

$$\vec{r}_\parallel = \vec{r}_\perp \times \vec{r}_N \tag{3.19}$$

The decomposition of the electric field vectors is now straightforward:

$$\vec{e}_V = (\vec{e}_V \bullet \vec{e}_\perp)\,\vec{e}_\perp + (\vec{e}_V \bullet \vec{e}_\parallel)\,\vec{e}_\parallel = V_\perp \vec{e}_\perp + V_\parallel \vec{e}_\parallel \tag{3.20a}$$

$$\vec{e}_H = (\vec{e}_H \bullet \vec{e}_\perp)\,\vec{e}_\perp + (\vec{e}_H \bullet \vec{e}_\parallel)\,\vec{e}_\parallel = H_\perp \vec{e}_\perp + H_\parallel \vec{e}_\parallel \tag{3.20b}$$

3.6 Transmitted and reflected fields

The transmission and reflection coefficients of the radome can be calculated following the method described in paragraph 2.2, the Transmission Line Equivalent. Assume an n-layer radome. Let's call Z(m) the equivalent impedance at the boundary between layer m and m+1. Then for $1 \leq m \leq n$, the equivalent impedance can be expressed as:

$$Z(m-1) = Z_m \frac{1+\rho(m)\exp(-2\gamma_m L_m)}{1-\rho(m)\exp(-2\gamma_m L_m)} \tag{3.21}$$

where

$Z_m = \sqrt{\mu_m/\varepsilon_m} = Z_{\text{free space}}/\sqrt{\varepsilon_{rm}}$ — the intrinsic or characteristic impedance of layer m (assumed $\mu_m = \mu_0$)

$\gamma_m = \alpha_m + j\beta_m$ — the propagation constant of layer m

$\beta_m = 2\pi/\lambda_m$ — the wavenumber of layer m

$\lambda_m = \lambda_0/\sqrt{\varepsilon_{rm}}$ — the wavelength in layer m

$\rho(m)$ is the reflection coefficient at boundary m which is the transition of layer m and m+1. The reflection coefficient is polarisation dependant in accordance with (2.2) and (2.3). For a multilayer radome these expressions become:

$$\rho_{\parallel}(m) = \frac{Z(m+1)\cos(\theta_{tm}) - Z_m \cos(\theta_{im})}{Z_m \cos(\theta_{im}) + Z(m+1)\cos(\theta_{tm})} \tag{3.22}$$

$$\rho_{\perp}(m) = \frac{Z(m+1)\cos(\theta_{im}) - Z_m \cos(\theta_{tm})}{Z_m \cos(\theta_{tm}) + Z(m+1)\cos(\theta_{im})} \tag{3.23}$$

Z(n+1) is the impedance of the outside free space.

The reflection coefficients at the inside of the radome are $\rho_{\parallel}(0)$ and $\rho_{\perp}(0)$. The reflected part of the incident wave is not transmitted and this is called reflection loss.

The transmission coefficients are related to the reflection coefficients by (2.5) and (2.6). The transmission coefficients of the whole radome are

$$\begin{aligned}\tau_{\parallel radome} &= \tau_{\parallel}(0)\prod_{m=1}^{n}\tau_{\parallel}(m)\exp(-\gamma_m L_m) \\ &= (\rho_{\parallel}(0)+1)\prod_{m=1}^{n}(\rho_{\parallel}(m)+1)\exp(-\gamma_m L_m)\end{aligned} \tag{3.24}$$

$$\begin{aligned}\tau_{\perp radome} &= \tau_{\perp}(0)\prod_{m=1}^{n}\tau_{\perp}(m)\exp(-\gamma_m L_m) \\ &= (\rho_{\perp}(0)+1)\prod_{m=1}^{n}(\rho_{\perp}(m)+1)\exp(-\gamma_m L_m)\end{aligned} \tag{3.25}$$

The transmitted fields are given by

$$\vec{t}_V = V_{\perp}.\tau_{\perp}.\vec{e}_{\perp} + V_{\parallel}\,\tau_{\parallel}\,\vec{e}_{\parallel} \tag{3.26a}$$

$$\vec{t}_H = H_{\perp}.\tau_{\perp}.\vec{e}_{\perp} + H_{\parallel}\,\tau_{\parallel}\,\vec{e}_{\parallel} \tag{3.26b}$$

The cross-polarisation caused by the transmission through the radome is calculated by

$$\vec{x}_V = \vec{t}_V \bullet \vec{e}_H \tag{3.27a}$$

$$\vec{x}_H = -\vec{t}_H \bullet \vec{e}_V \tag{3.27b}$$

Since the wavelength in a dielectric material is different from the wavelength in free space, the phase of the transmitted signal changes. To get a correct value for the phase change, the phase of the transmission coefficient has to be corrected for the phase of the transmission through a similar layer of air.

4. Design and simulated results for the PHARUS radome

PHARUS is a full polarimetric system with a high polarisation purity. So the additional cross-polarisation due to the transmission through the radome is an important design parameter. Also important is the loss of signal since loss reduces the detection range of the radar. Loss can be caused by reflection at the radome (reflection loss) and absorption in the radome (transmission loss). Measurements [4] have shown that Dyneema-composites have a very low loss tangent ($\tan(\delta) < 0.02$) so the transmission loss can be neglected. The phase shift caused by the radome is of minor importance. The shift is only dependant on the path through the radome and that is not polarisation sensitive. It can only cause some distortion when there is a strong gradient over the antenna beam.

The region of interest is determined by the scan angle and the beamwidth. For PHARUS this is:

Azimuth:

$$\left.\begin{array}{l}\text{scanangle: } 20^\circ \\ \theta_{3dB} \approx 3.5^\circ\end{array}\right\} \Rightarrow \quad Az < \text{scanangle} + \tfrac{1}{2}\theta_{3dB} = 22^\circ$$

Elevation:

$$\left.\begin{array}{l}\text{scanangle: } 15^\circ \\ \theta_{3dB} \approx 25^\circ\end{array}\right\} \Rightarrow \quad El < \text{scanangle} + \tfrac{1}{2}\theta_{3dB} = 28^\circ$$

The design parameters are in principle the number of layers of the radome, the material of the layers, the thickness of the layers and the shape of the radome. Multilayer radomes are hard to construct. From a mechanical point of view a single layer is preferred. The choice of materials is also dependant on the mechanical properties. From Dyneema it was known that it had good mechanical properties and from earlier measurements [4] the electrical properties are well-known. Especially the low loss tangent is attractive. The shape of the radome is more or less dictated by the antenna. Since this is a long and narrow configuration, a cylindrical shape is a natural choice. So the remaining design parameters are the thickness of the radome and the radius of the cylinder with the restriction that the maximum allowable height above the frame is 100 mm.

In general there are two design approaches. The first one aims for a radome as thin as possible. The second approach is to make the radome thickness half of the wavelength (in the dielectric layer). From transmission line theory it is well-known that a half lambda line is transparent regardless of its impedance. In appendix A, the results of the simulations for a range of radome thicknesses and radii are shown. The simulations lead to the following conclusions:

- the cross-polar performance is merely determined by the shape of the radome.
- the cross-polar deterioration is almost identical for both polarisations.
- the reflection loss is primarily dependant on the radome thickness.

These results become obvious if multiple bounces inside the radome are neglected. Obviously they do not play an important role in this case.

The best performance can be reached by a half lambda radome, shaped as half a cylinder with the antenna in its centre. Unfortunately, this radome exceeds the allowed height above the frame. Mechanical strength considerations dictated that the radome should be at least 4 mm thick. On the other hand, 4 mm is preferred above 19 mm for weight reduction. So a 4 mm thick radome with a maximal height above the frame seems the best achievable compromise.

According to the simulations, the reflection loss should be less than 0.4 dB and the extra cross-polar contribution caused by the radome is expected to be less than -40 dB. At a level of -25 dB, which is the expected cross-polar performance of the antenna, this can yield a maximum deterioration of 1.5 dB. This is acceptable. Fig. 4.1 to 4.5 show the simulated performance of the final PHARUS radome.

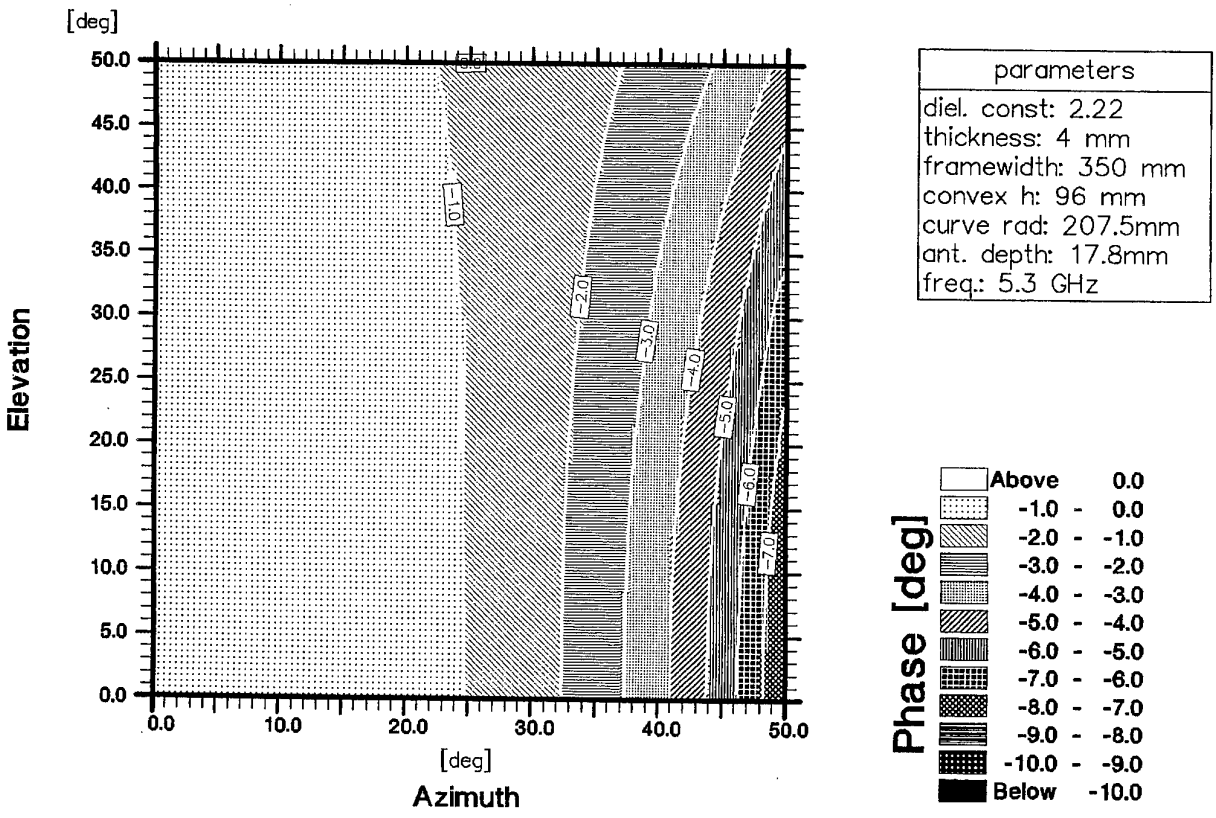

Figure 4.1: Additional phase shift by PHARUS radome

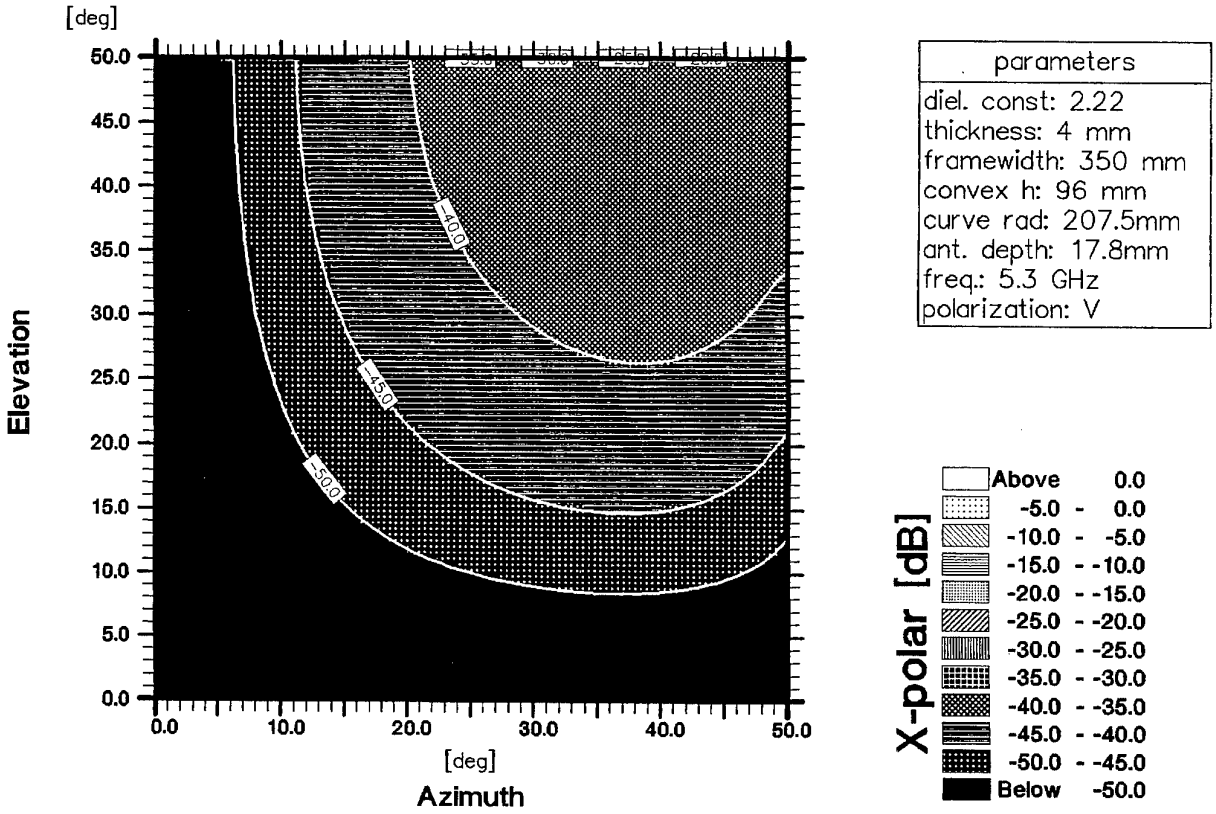

Figure 4.2: Additional cross-polarisation by PHARUS radome, vertical polarisation

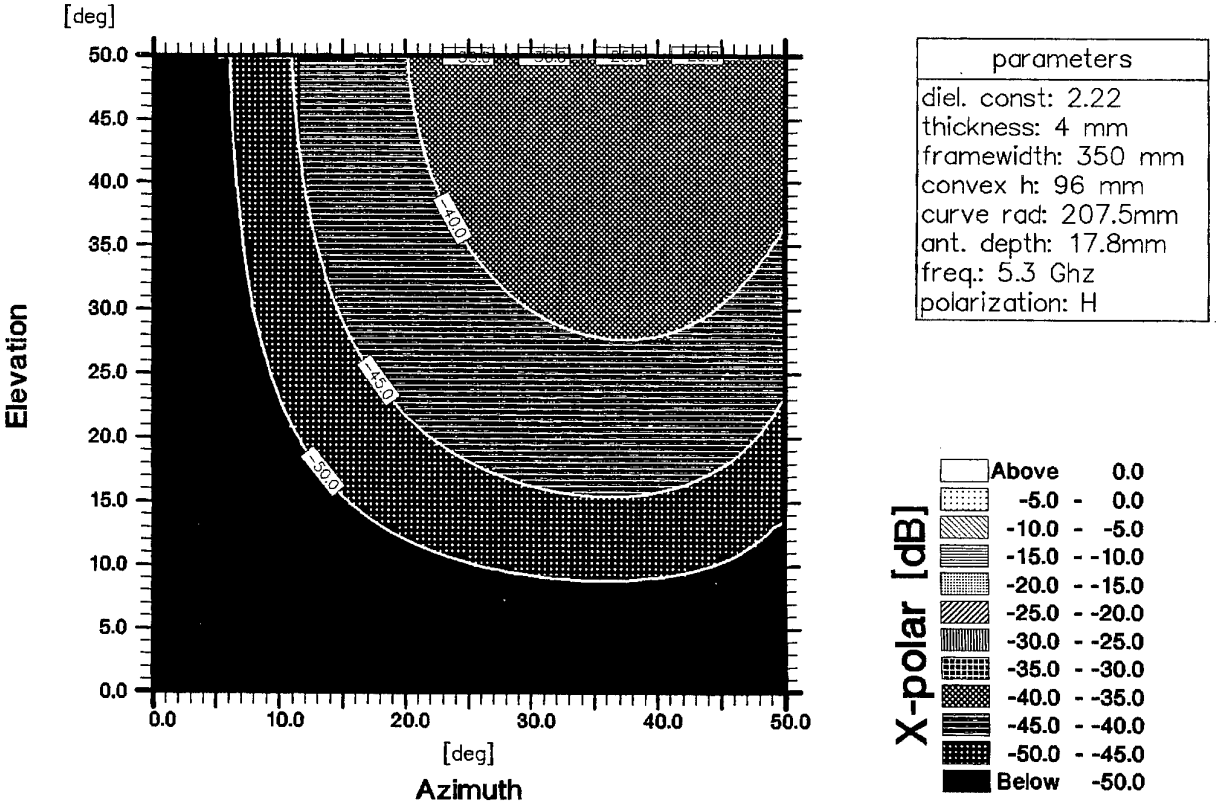

Figure 4.3: Additional cross-polarisation by PHARUS radome, horizontal polarisation

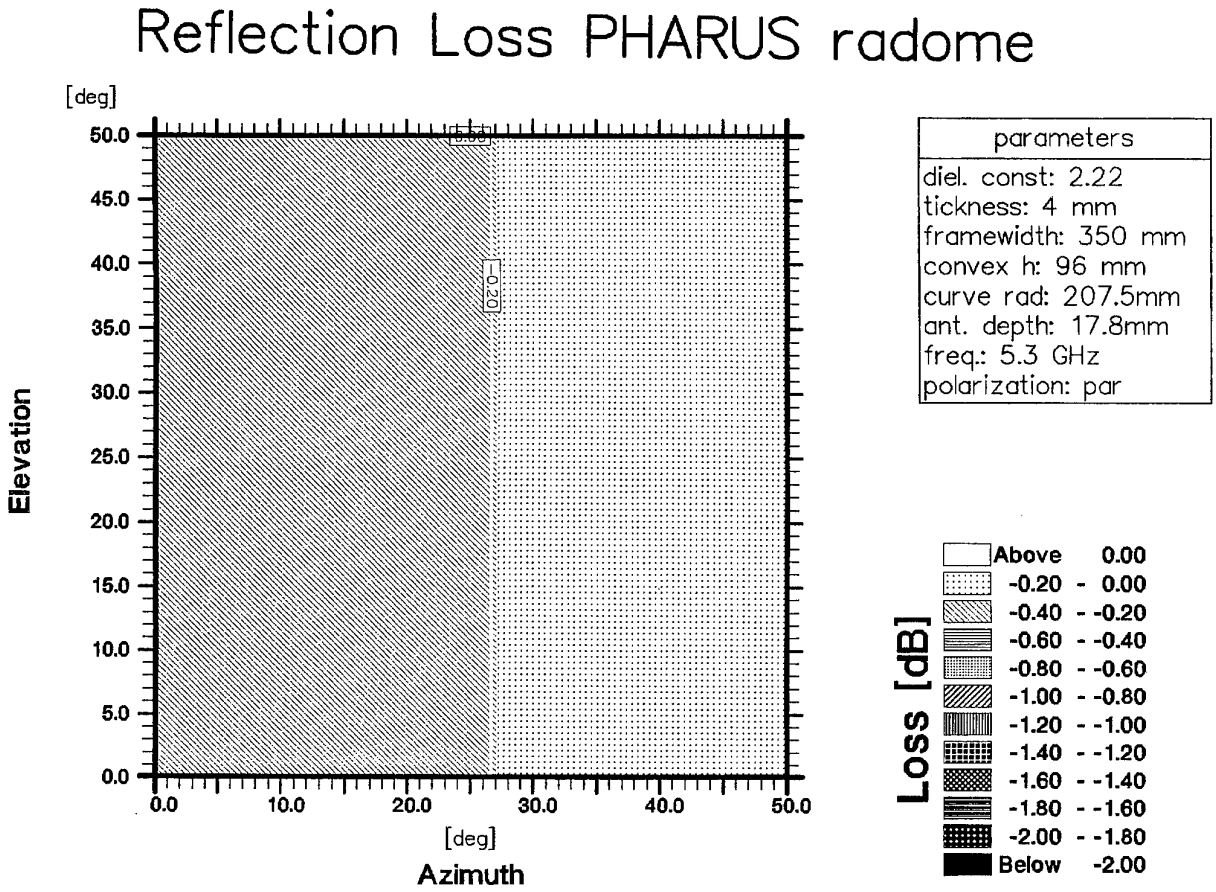

Figure 4.4: Return loss of PHARUS radome, parallel components

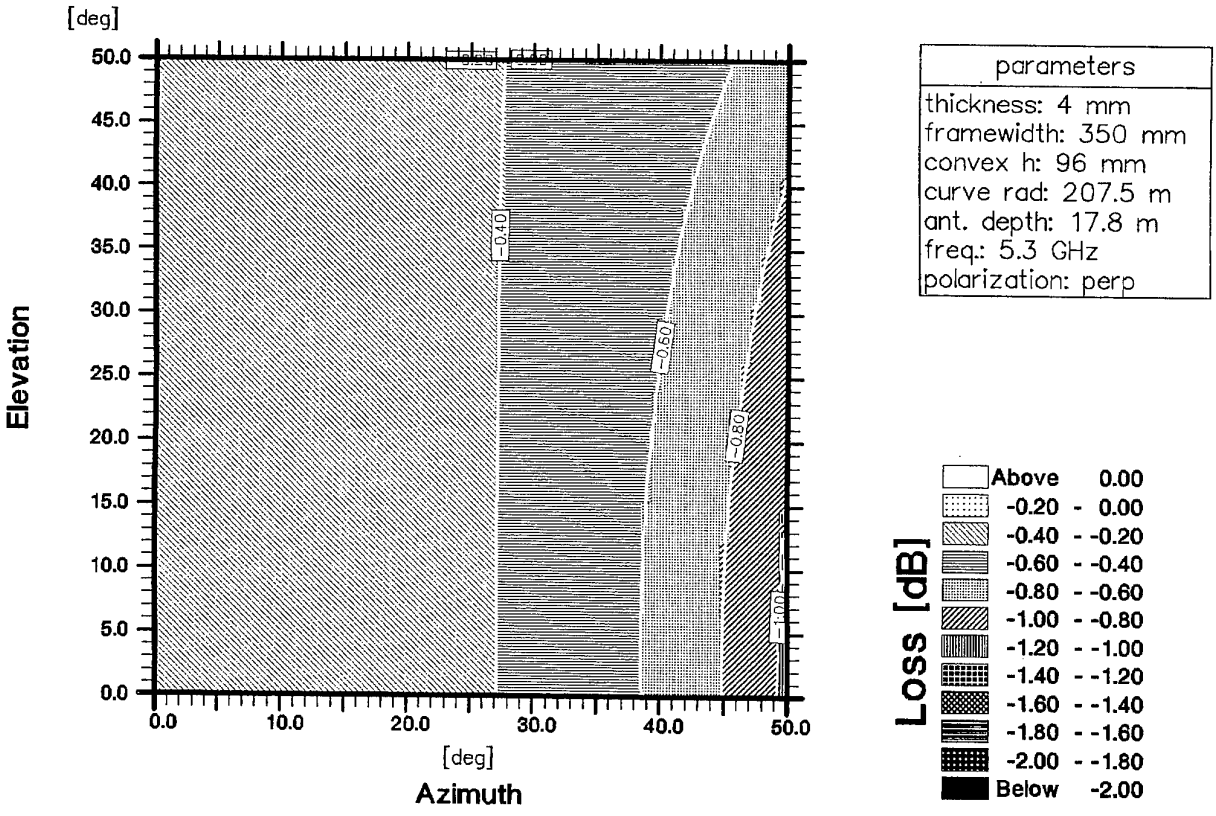

Figure 4.5: Return loss of PHARUS radome, perpendicular components

5. Realisation and verification

5.1 Construction

For the construction of the PHARUS radome, a mould has been made. On this mould, alternately 17 layers of Dyneema texture and 18 layers of Stamylex PE film have been applied. Finally the radome was hardened for 60 minutes in a so-called autoclave under 60 bar pressure and a temperature of 145 °C.

5.2 Measurements

The radome has been measured on the TNO-FEL Near Field Antenna range. A Standard Gain horn has been used as illuminator. Due to the construction of the PHARUS body it was unpractical to measure the PHARUS antenna with and without radome. The set-up is shown in figure 5.1.

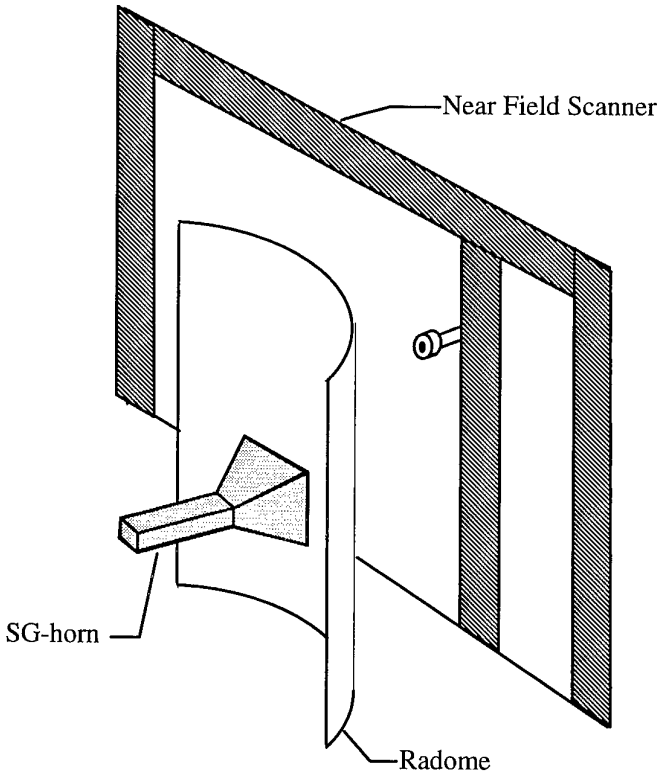

Figure 5.1: Measurement set-up for radome test.

The Standard Gain horn has been measured with and without radome. Figure 5.2 and 5.3 show a comparison of the measurements with and without radome. The goal of the measurement has been a test of the radome performance so not much effort has been put in aligning the Standard Gain horn. The measurements verify that the radome does not spoil the cross-polar performance of the antenna which means that it is suitable for use in the PHARUS system.

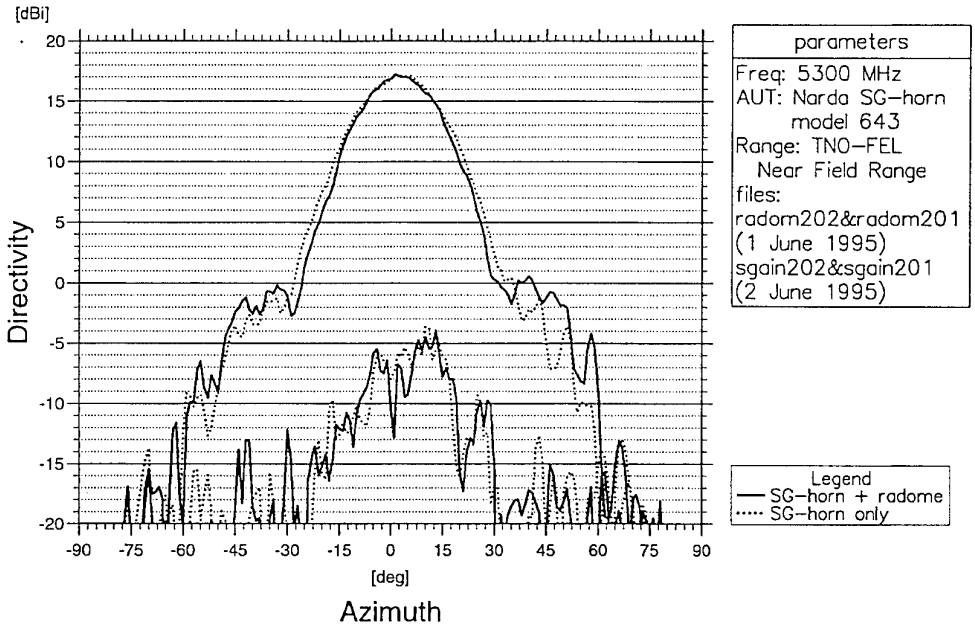

Figure 5.2: Comparison of Standard Gain horn antenna patterns with and without radome, azimuth plane

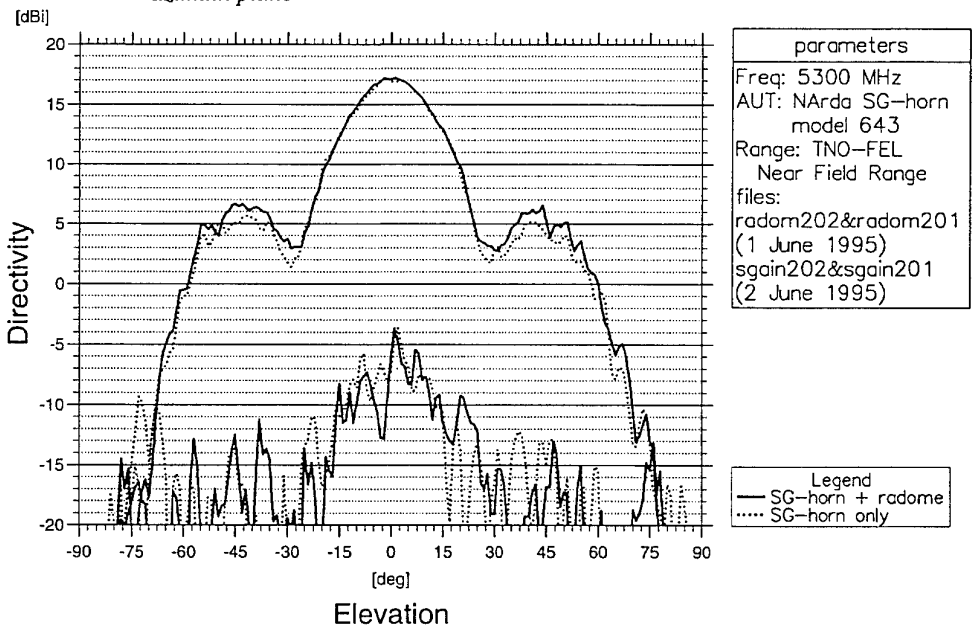

Figure 5.3: Comparison of Standard Gain horn antenna patterns with and without radome, elevation plane

6. Conclusions

- The analysis method, based on Single Ray Tracing and Transmission Line Equivalence is useful for radome analysis.
- Dyneema-composites are very suitable for radomes due to their high mechanical strength and low loss tangent.
- The cross-polar performance is mainly determined by the shape of the radome.
- The cross polar deterioration is almost identical for both polarisations.
- The reflection loss is primarily dependant on the radome thickness.
- A single layer cylindrical radome with a radius of 207.5 mm and a thickness of 4 mm is the best achievable compromisebetween electrical and mechanical requirements.

7. References

[1] PHARUS eindrapport

[2] Hirsch H.L., D.C. Grove, "Practical Simulation of Radar Antennas and Radomes", Artech House 1987, ISBN 0-89006-237-4

[3] Ludwig A.C., "The definition of Cross Polarization", IEEE Trans. A&P, Vol. 21, no. 1, jan. 1973, pp. 116-119

[4] Heemskerk H.J.M., "Reflection and Transmission Properties of three Dyneema composites at X-band", TNO Physics and Electronics Laboratory, report FEL-90-C108, march 1990.

8. Signature

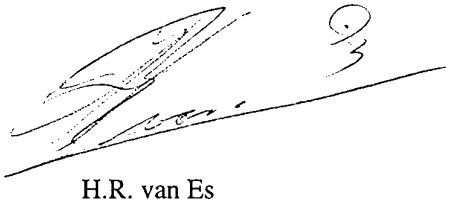

H.R. van Es
Group leader

M.H.A. Paquay
Author

Appendix A Results of the simulations

Table A.1 shows the combinations of parameters for which the performance has been simulated.

*Table A.1: Overview of simulations (The half cylinder radomes, marked with an * are higher than permitted. They are included for comparison)*

radome thickness [mm]	height above the frame [mm]	inside radius of the radome [mm]	Frame width [mm]	antenna depth (behind frame aperture) [mm]	remarks	Figures
4	0.1	153125	350	16.6	flat radome	A.1
4	175*	175	350	0	half cylinder	A.2
2	98	205	350	16.6	max. height	A.3
4	96	207.5	350	16.6	max. height	A.4
6	94	210	350	16.6	max. height	A.5
10	90	215	350	16.6	max. height	A.6
19	81	230	350	16.6	max. height half lambda	A.7
19	175*	175	350	0	half cylinder half lambda	A.8

For the combinations of table A.1, the following plots have been generated:

- the additional phase shift of the radome (polarisation independent)
- the additional cross-polarisation for one polarisation (the other polarisation happens to have an identical performance)
- the reflection loss for both polarisations is given.

By comparison there can be seen that the cross-polarisation is merely determined by the shape of the radome. The reflection loss is primarily determined by the radome thickness. A rapid increase can be noticed by comparing the 2, 4 and 6 mm radome (figures A.3, A.4 and A.5). Notice also the excellent behaviour of the half lambda radomes.

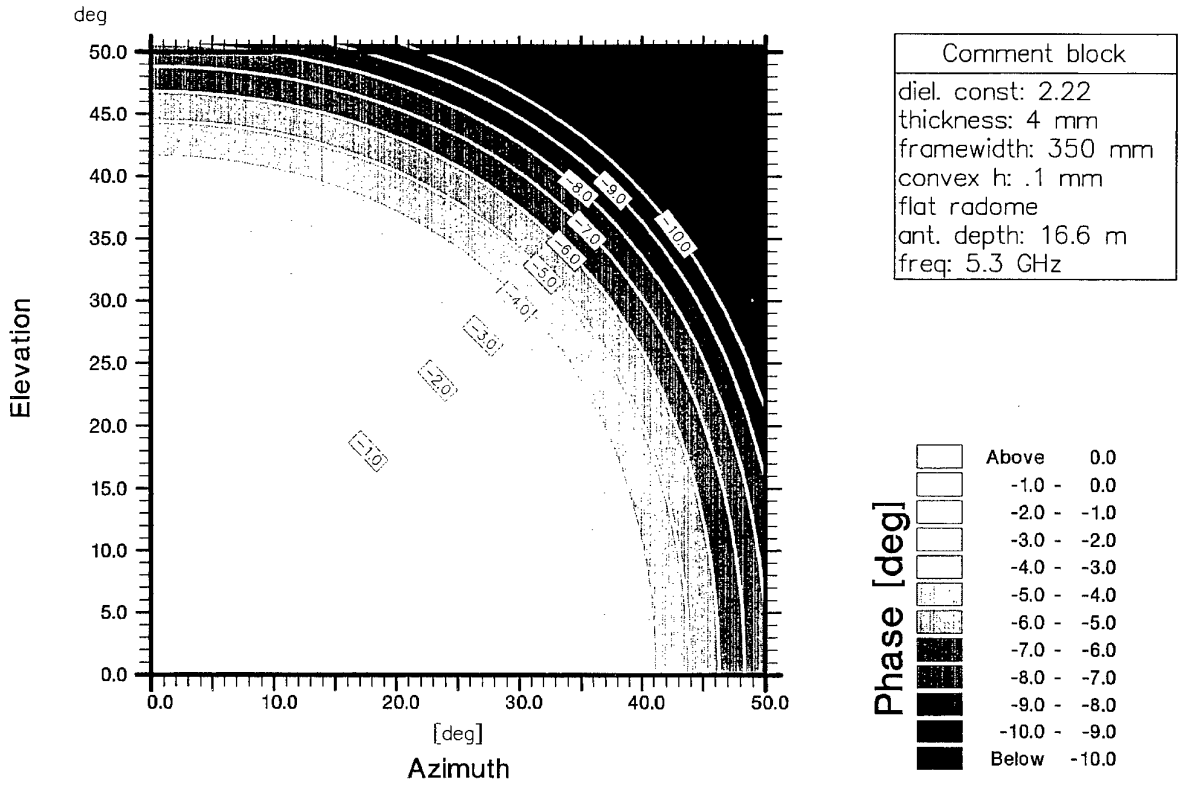

Figure A.1.a: Additional phase shift a flat radome of 4 mm thickness

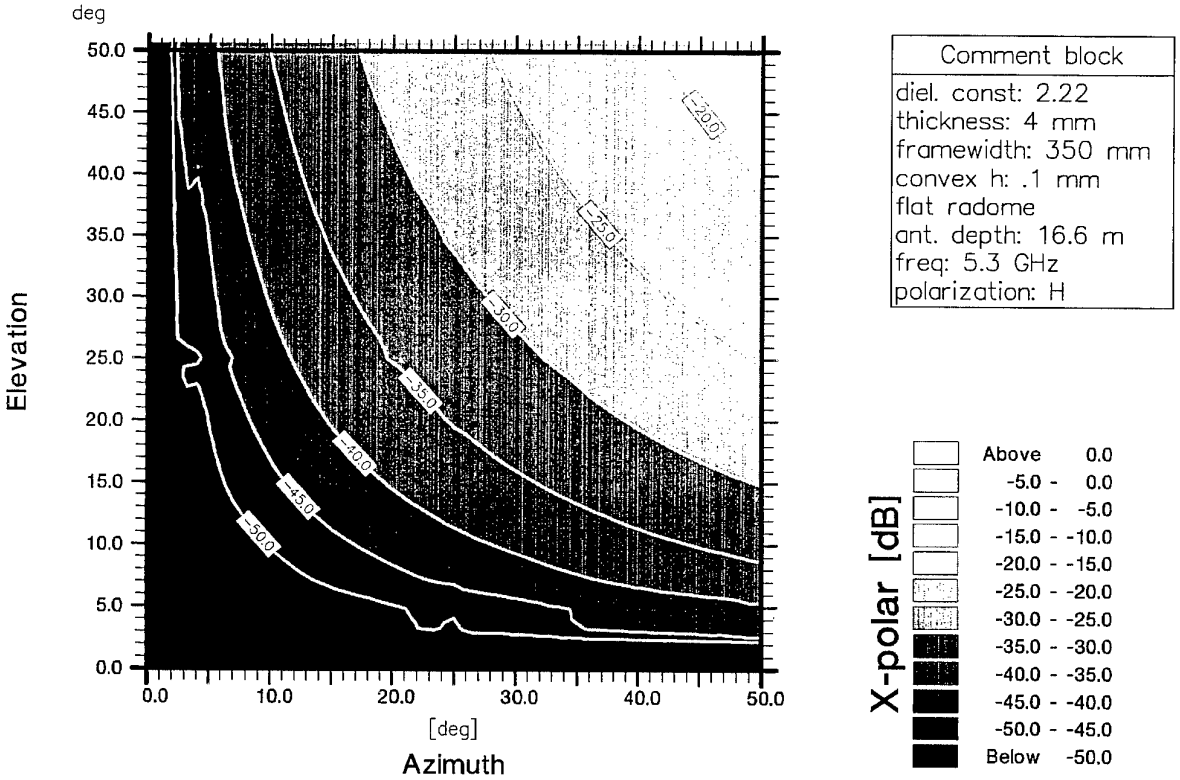

Figure A.1.b: Additional cross-polarisation of a flat radome of 4 mm thickness (the cross-polarisation performance is identical for both horizontal and vertical polarisation)

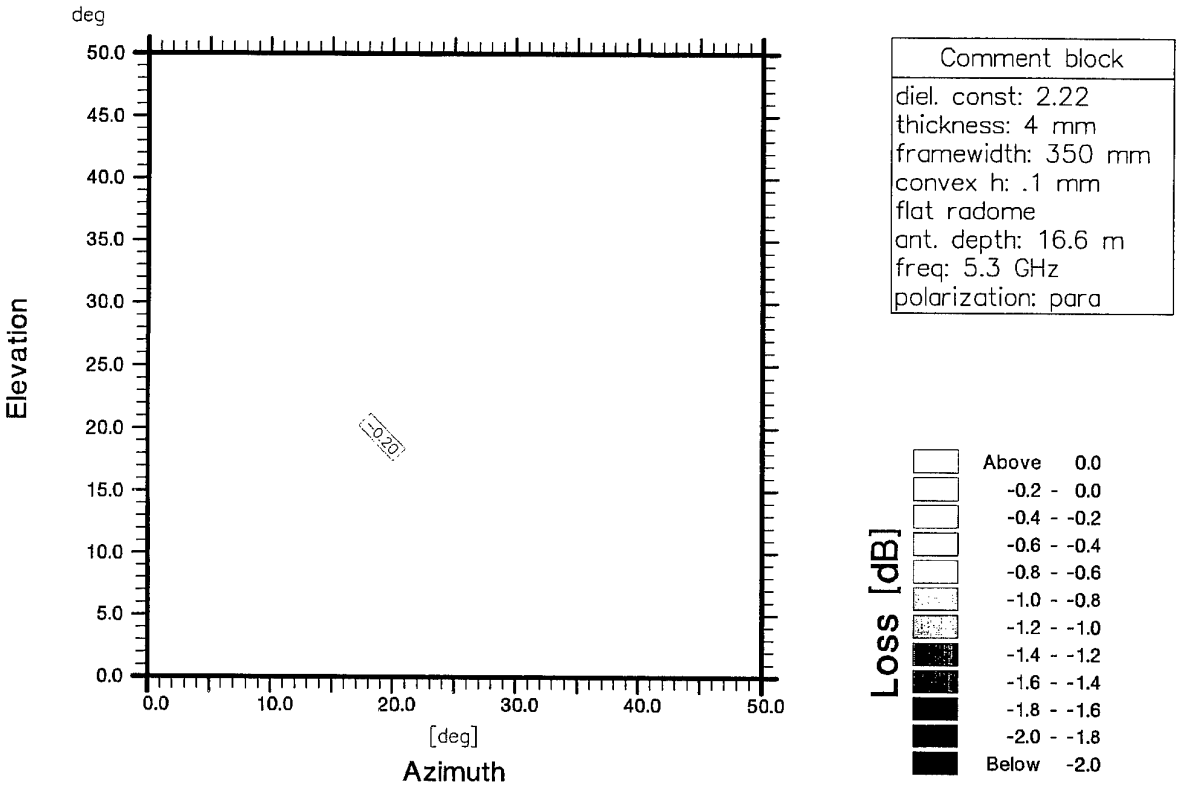

Figure A.1.c: Return loss of a flat radome of 4 mm thickness, parallel components

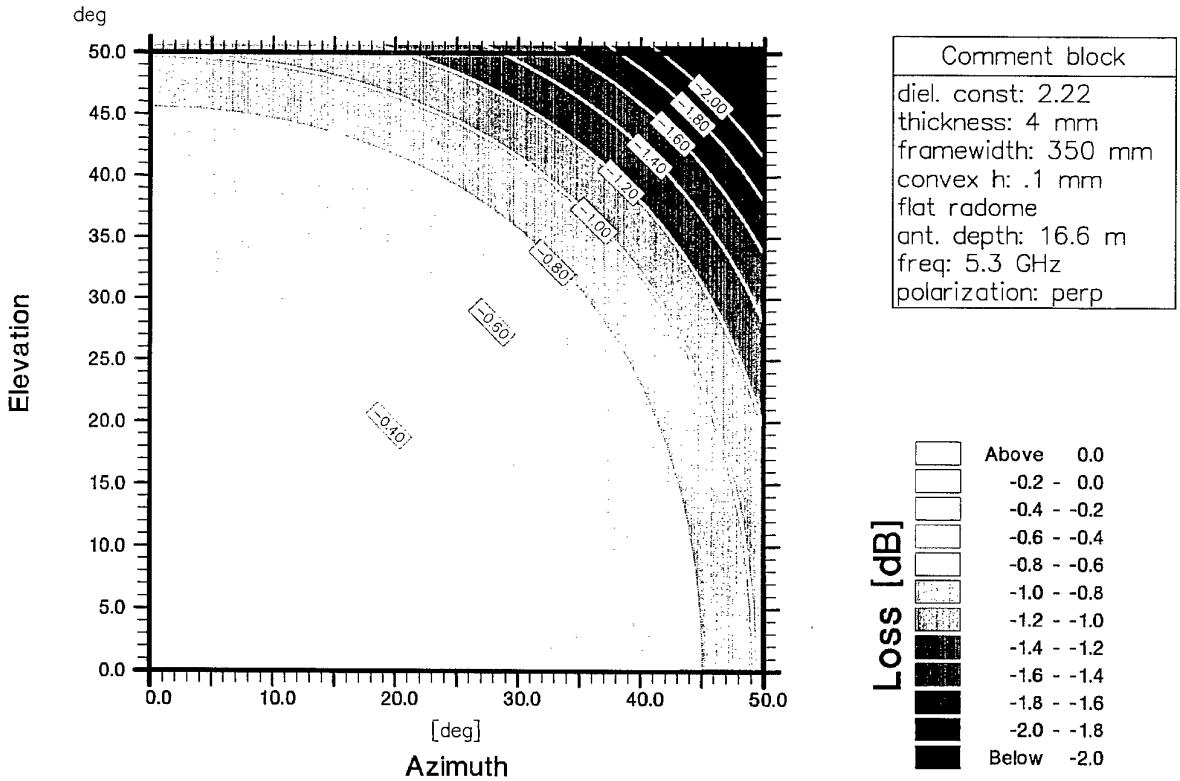

Figure A.1.d: Return loss of a flat radome of 4 mm thickness, perpendicular components

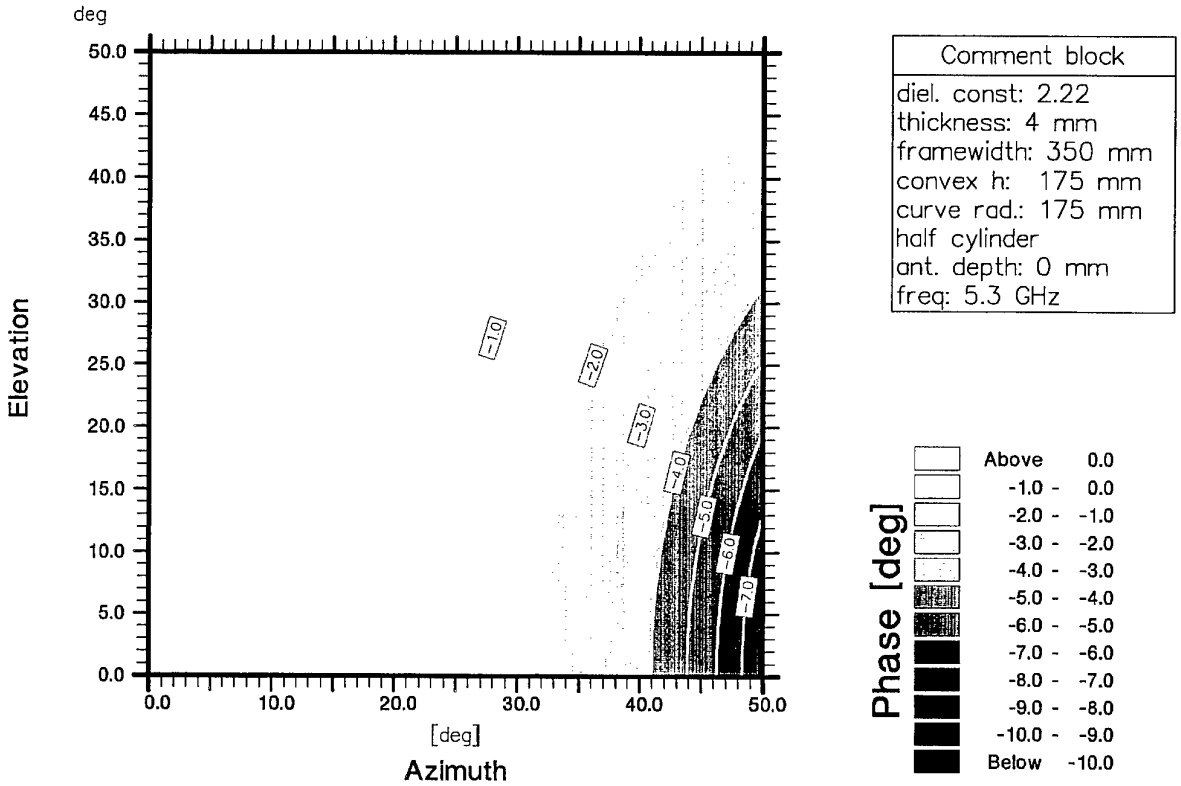

Figure A.2.a: Additional phase shift a half cylinder radome of 4 mm thickness

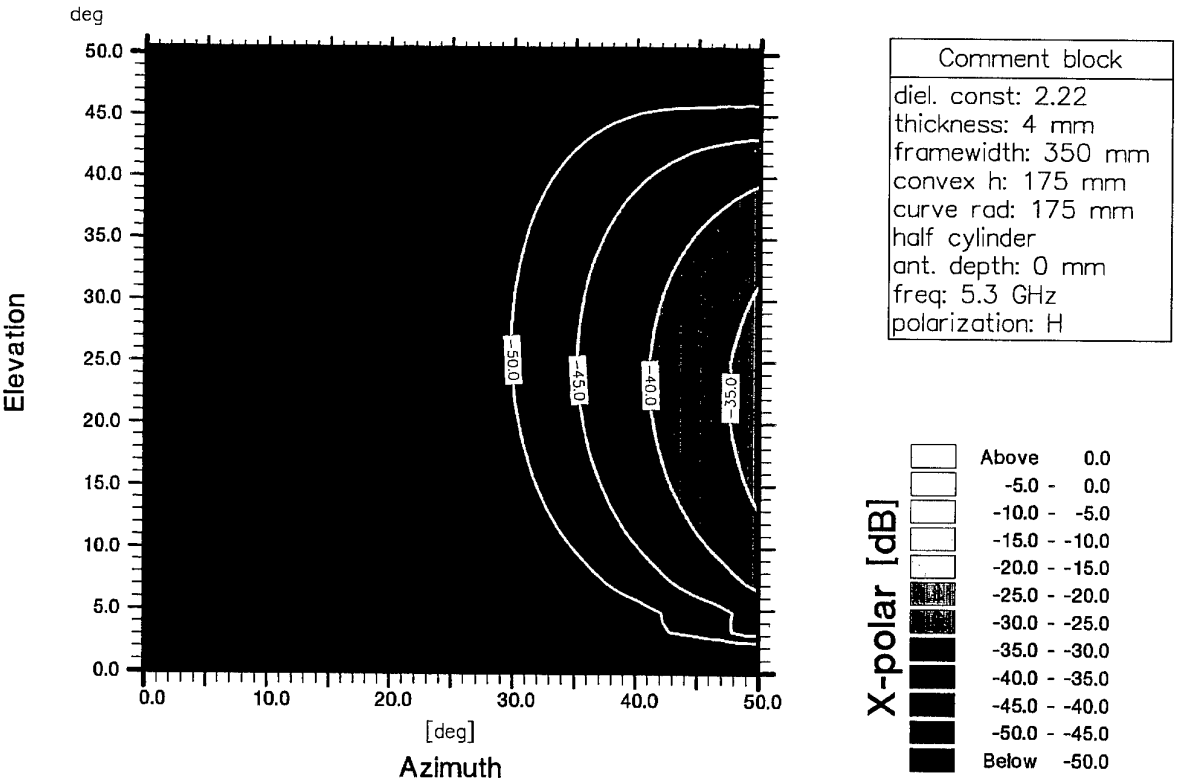

Figure A.2.b: Additional cross-polarisation of a half cylinder radome of 4 mm thickness (the cross-polarisation performance is identical for both horizontal and vertical polarisation)

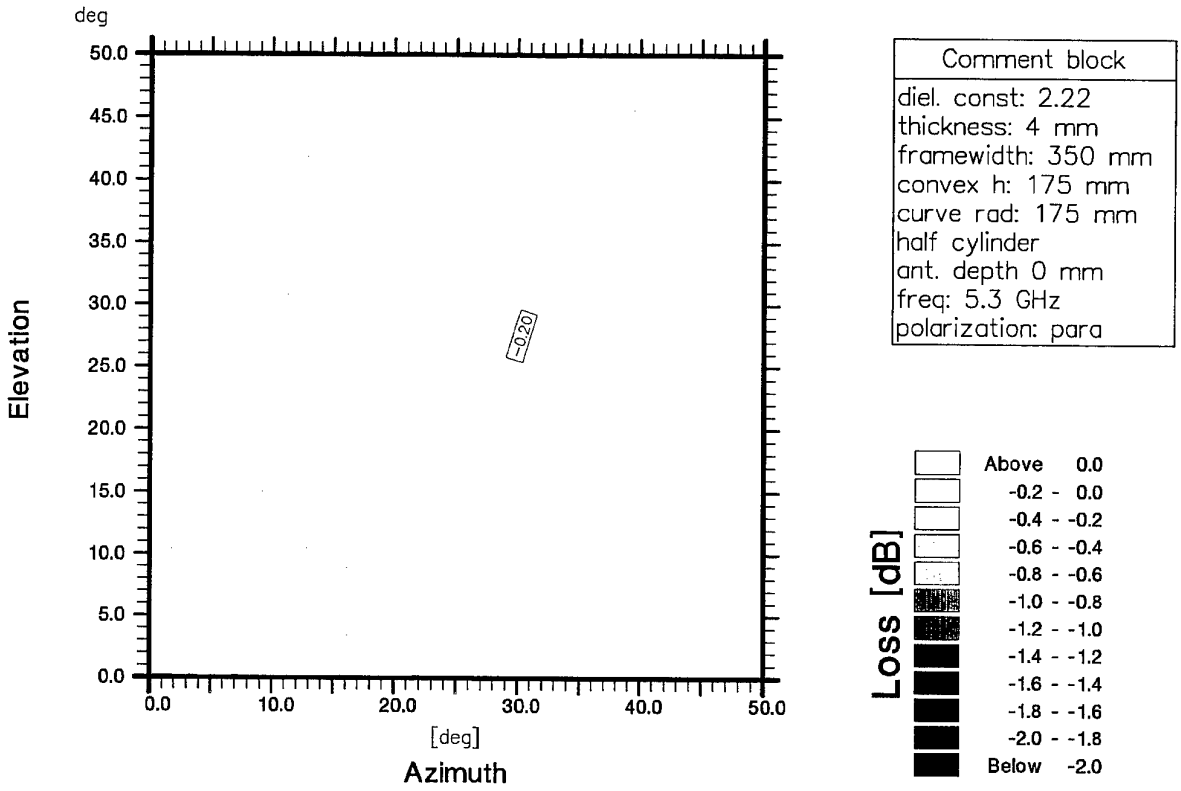

Figure A.2.c: Return loss of a half cylinder radome of 4 mm thickness, parallel components

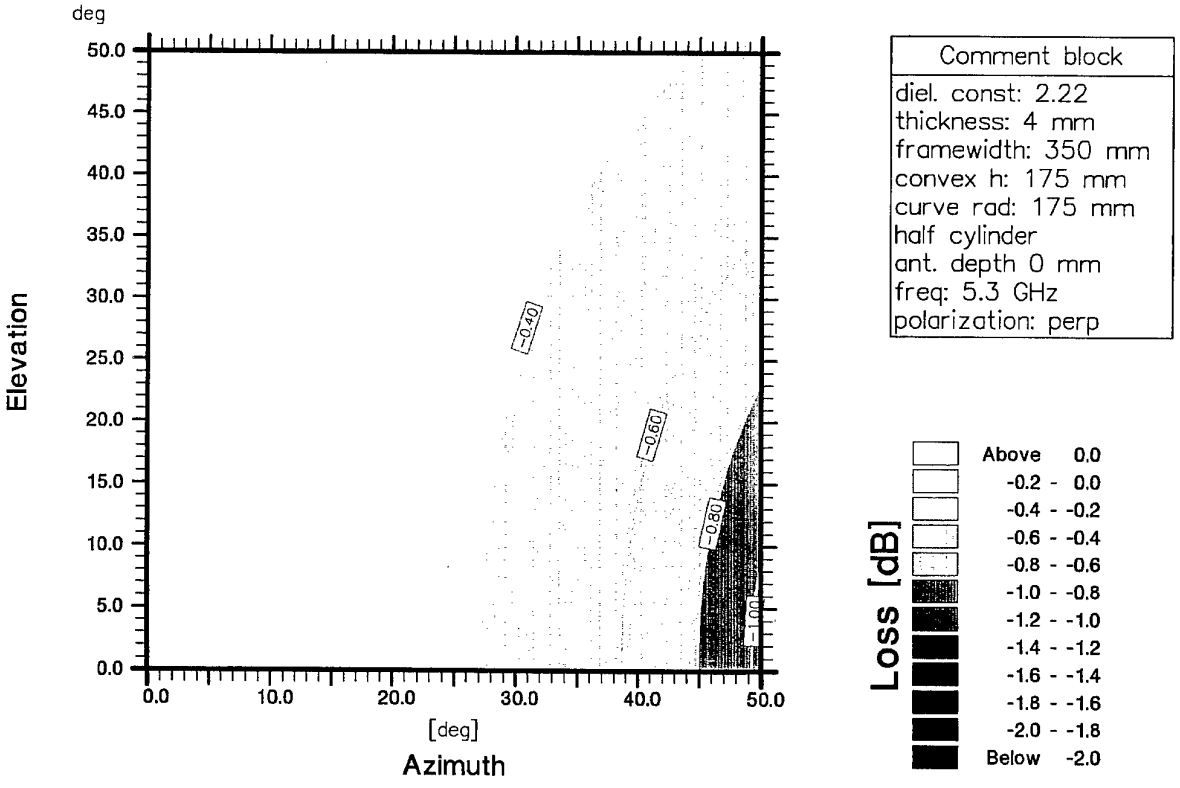

Figure A.2.d: Return loss of a half cylinder radome of 4 mm thickness, perpendicular components

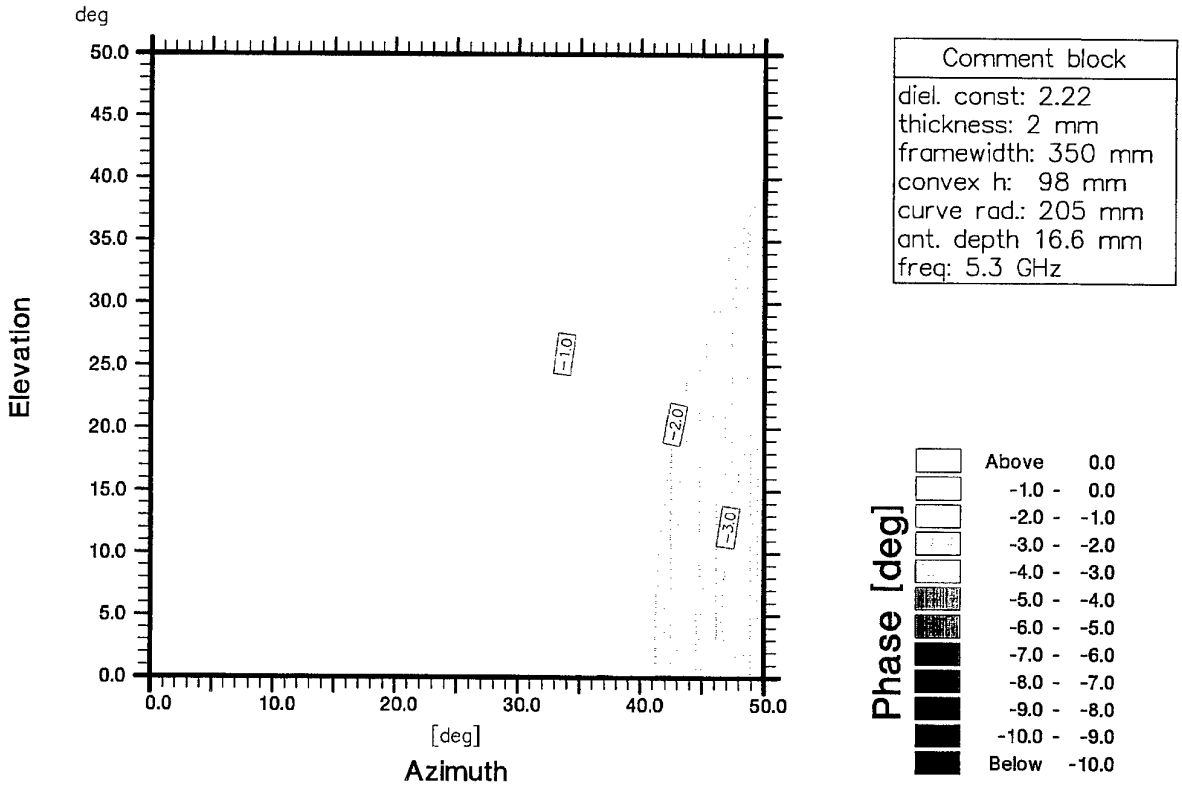

Figure A.3.a: Additional phase shift a radome of 2 mm thickness, max. height

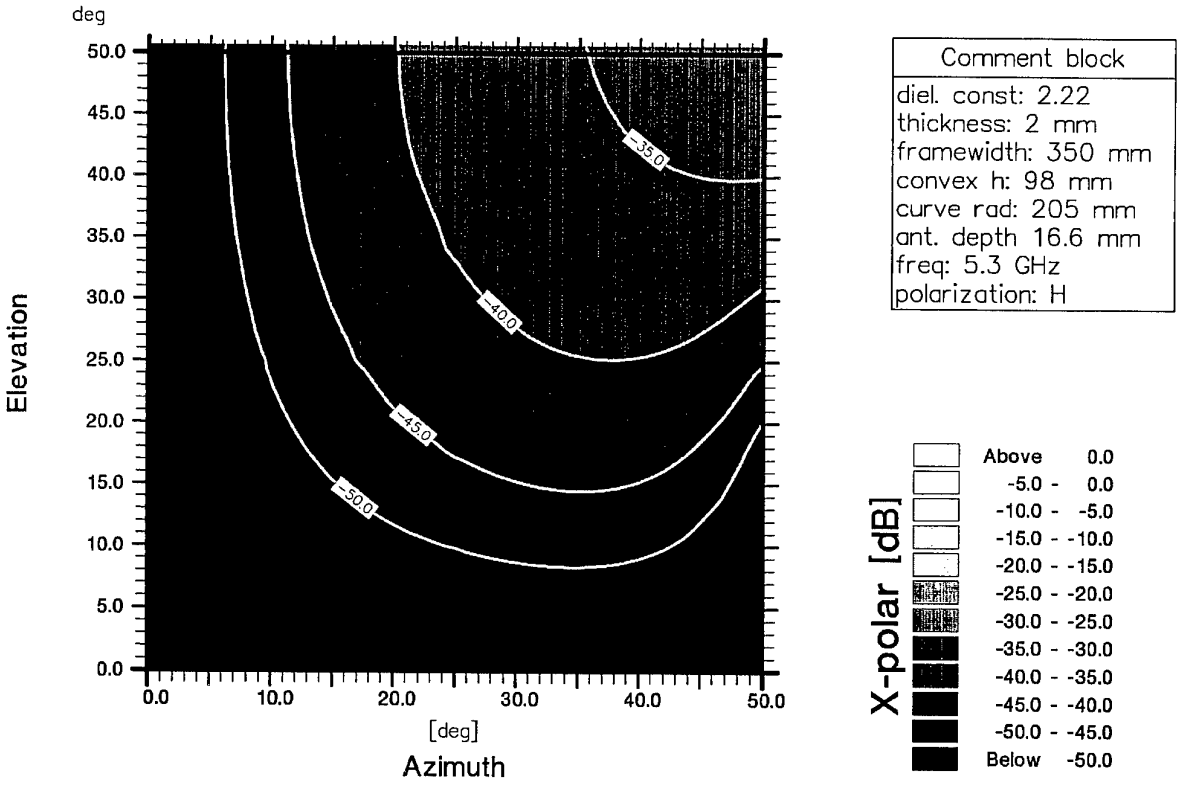

Figure A.3.b: Additional cross-polarisation of a radome of 2 mm thickness, max. height (the cross-polarisation performance is identical for both horizontal and vertical polarisation)

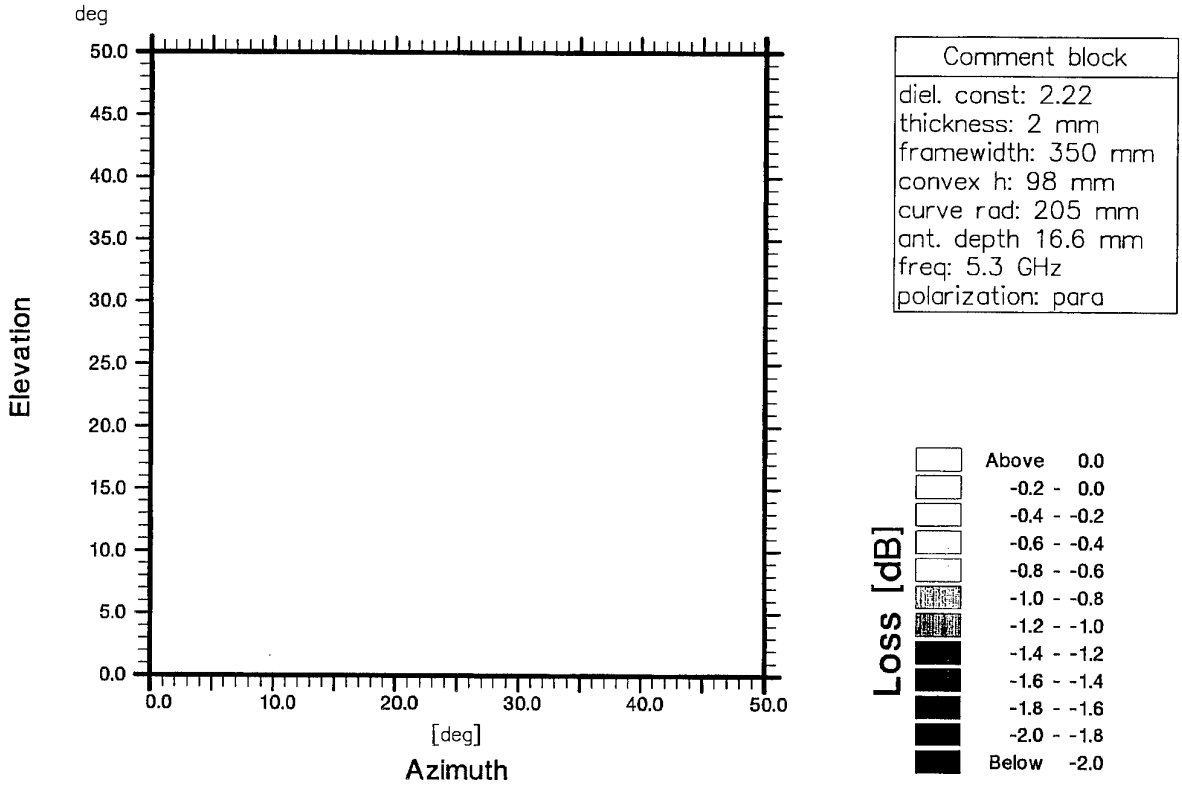

Figure A.3.c: Return loss of a radome of 2 mm thickness, max. height, parallel components

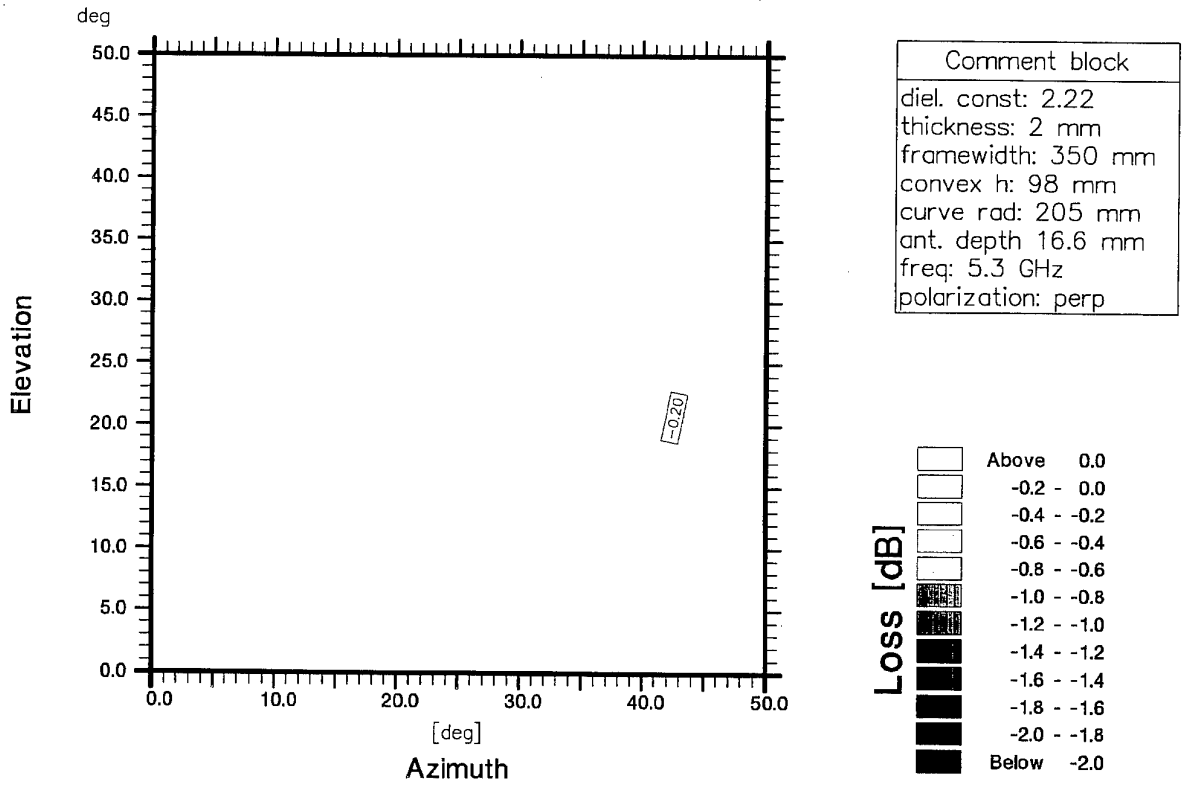

Figure A.3.d: Return loss of a radome of 2 mm thickness, max. height perpendicular components

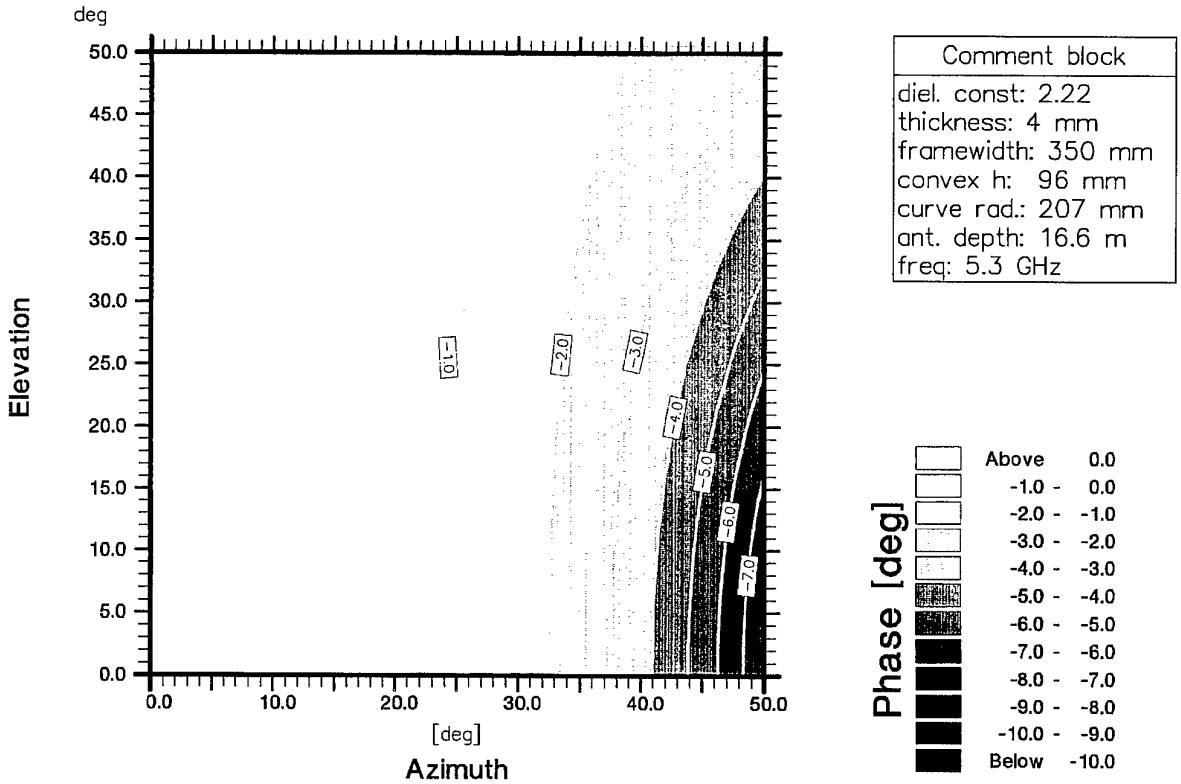

Figure A.4.a: Additional phase shift a radome of 4 mm thickness, max. height (final PHARUS radome)

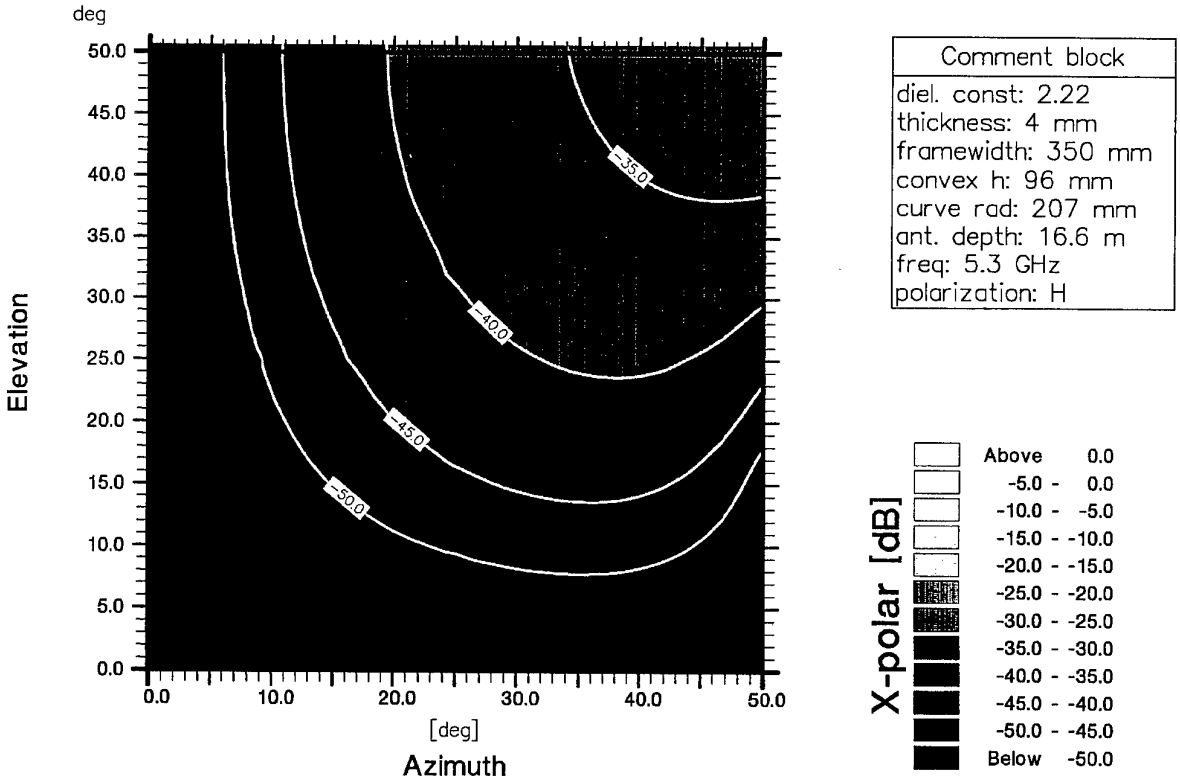

Figure A.4.b: Additional cross-polarisation of a radome of 4 mm thickness, max. height (final PHARUS radome) (the cross-polarisation performance is identical for both horizontal and vertical polarisation)

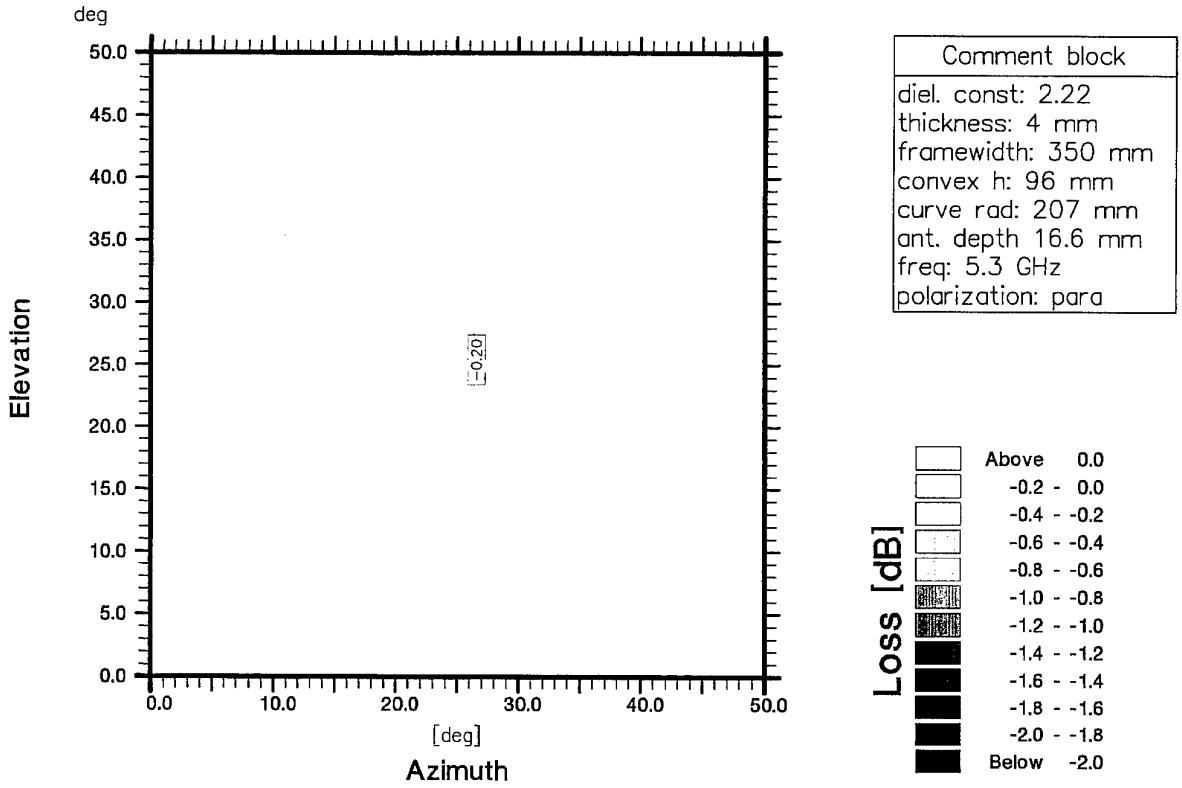

Figure A.4.c: Return loss of a radome of 4 mm thickness, max. height, parallel components (final PHARUS radome)

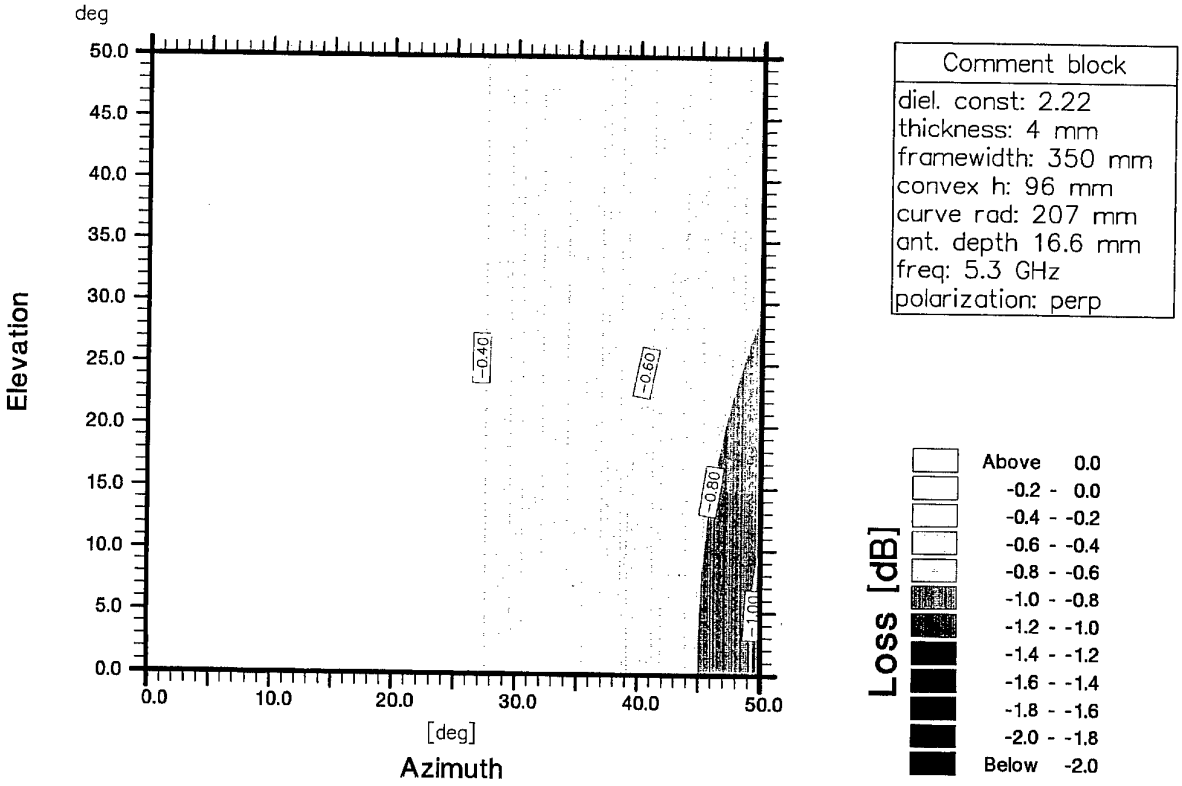

Figure A.4.d: Return loss of a radome of 4 mm thickness, max. height perpendicular components (final PHARUS radome)

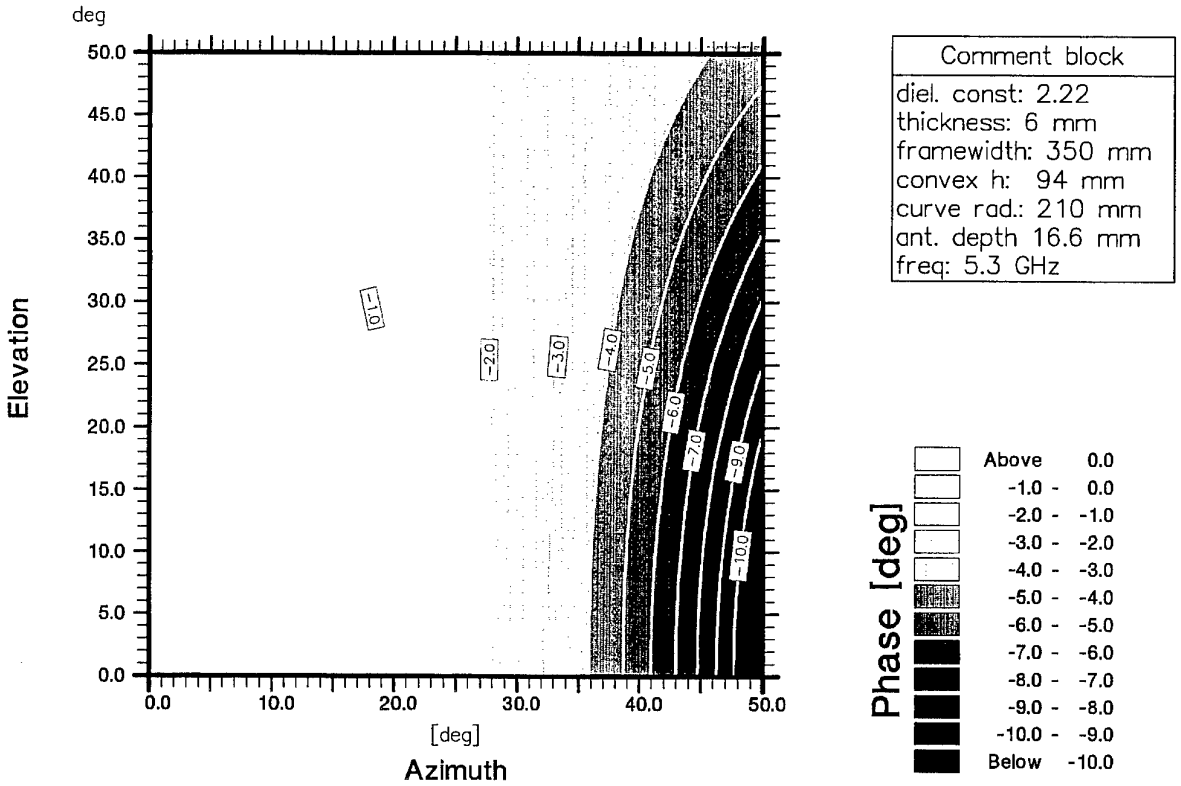

Figure A.5.a: Additional phase shift a radome of 6 mm thickness, max. height

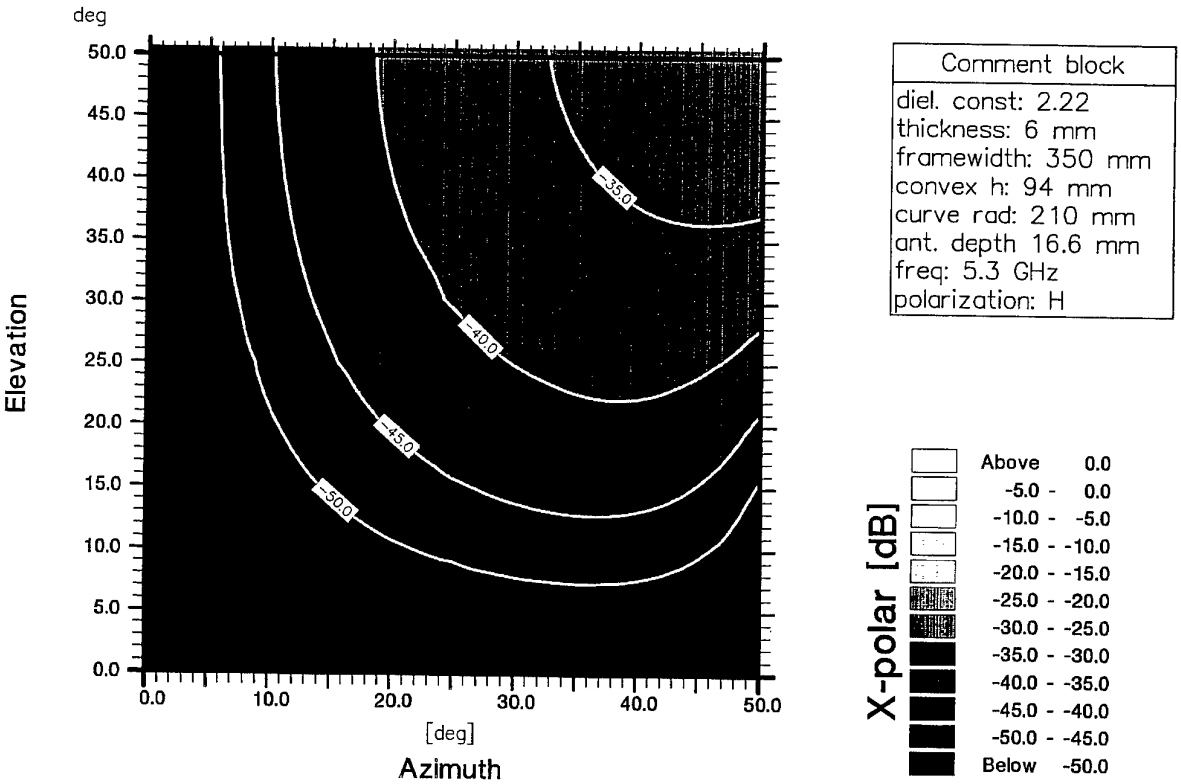

Figure A.5.b: Additional cross-polarisation of a radome of 6 mm thickness, max. height (the cross-polarisation performance is identical for both horizontal and vertical polarisation)

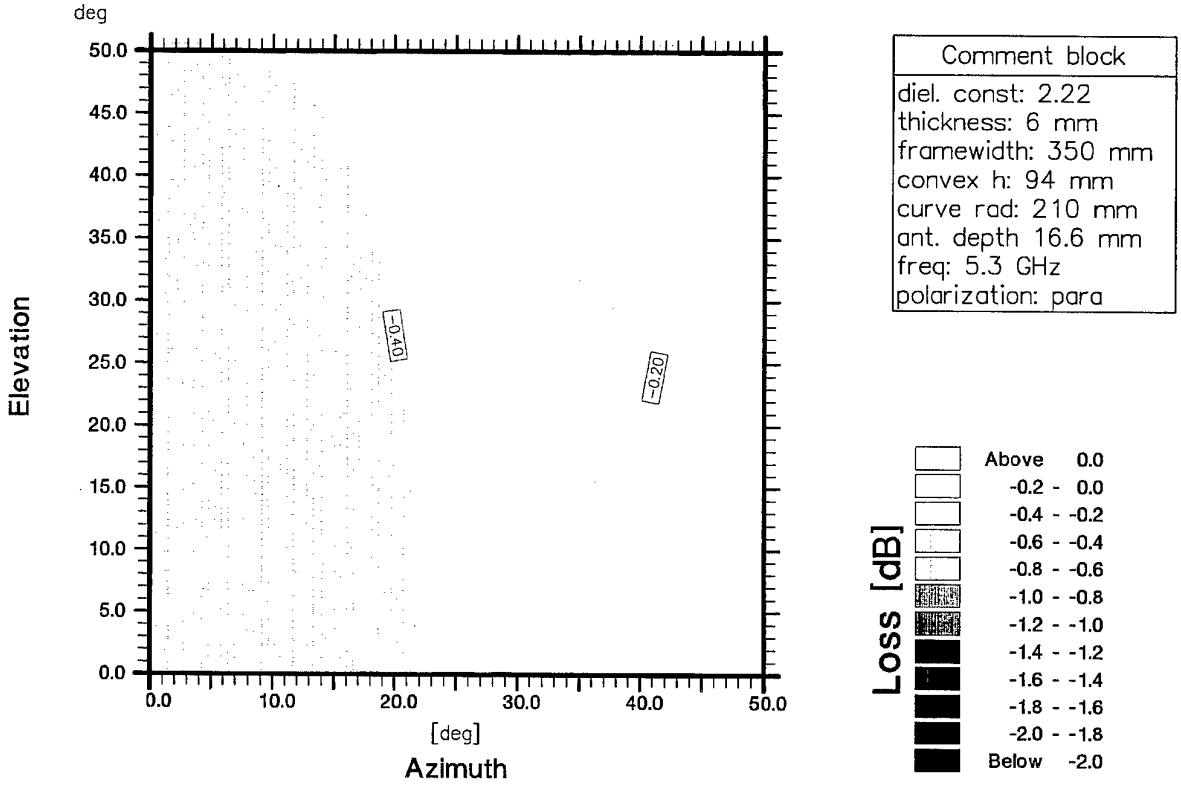

Figure A.5.c: Return loss of a radome of 6 mm thickness, max. height, parallel components

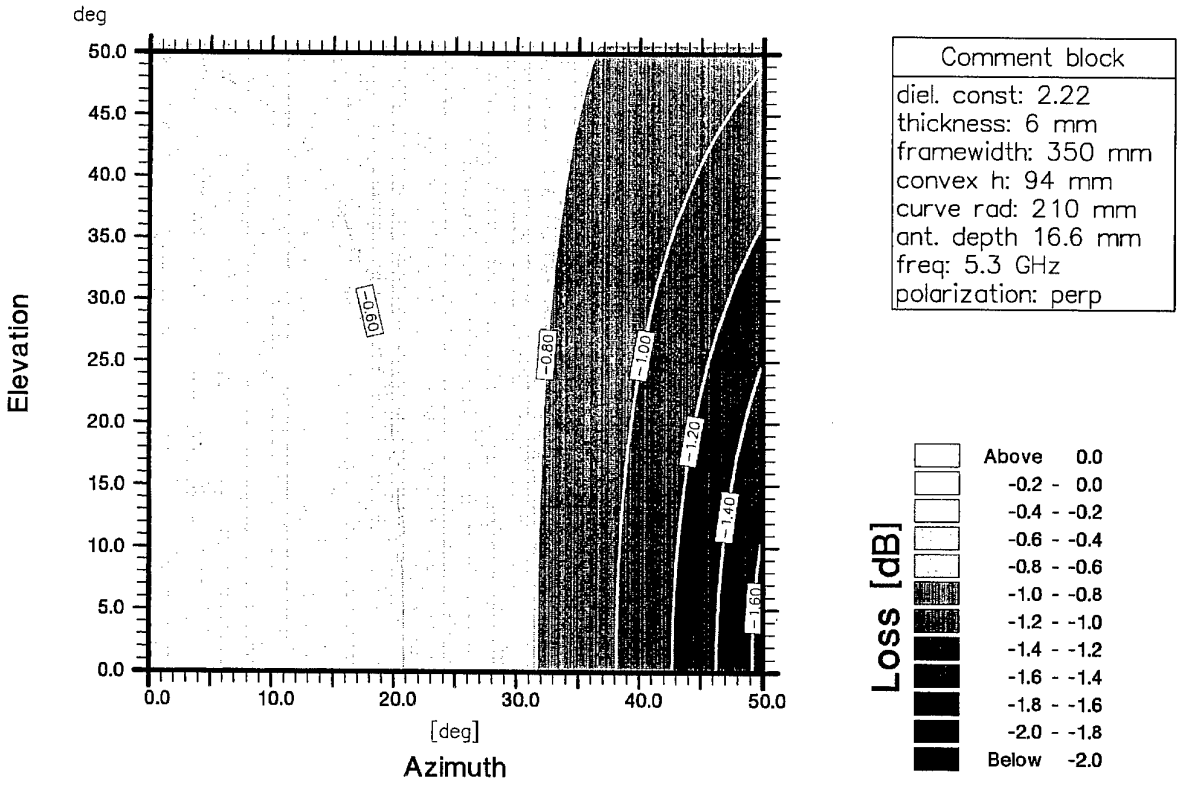

Figure A.5.d: Return loss of a radome of 6 mm thickness, max. height, perpendicular components

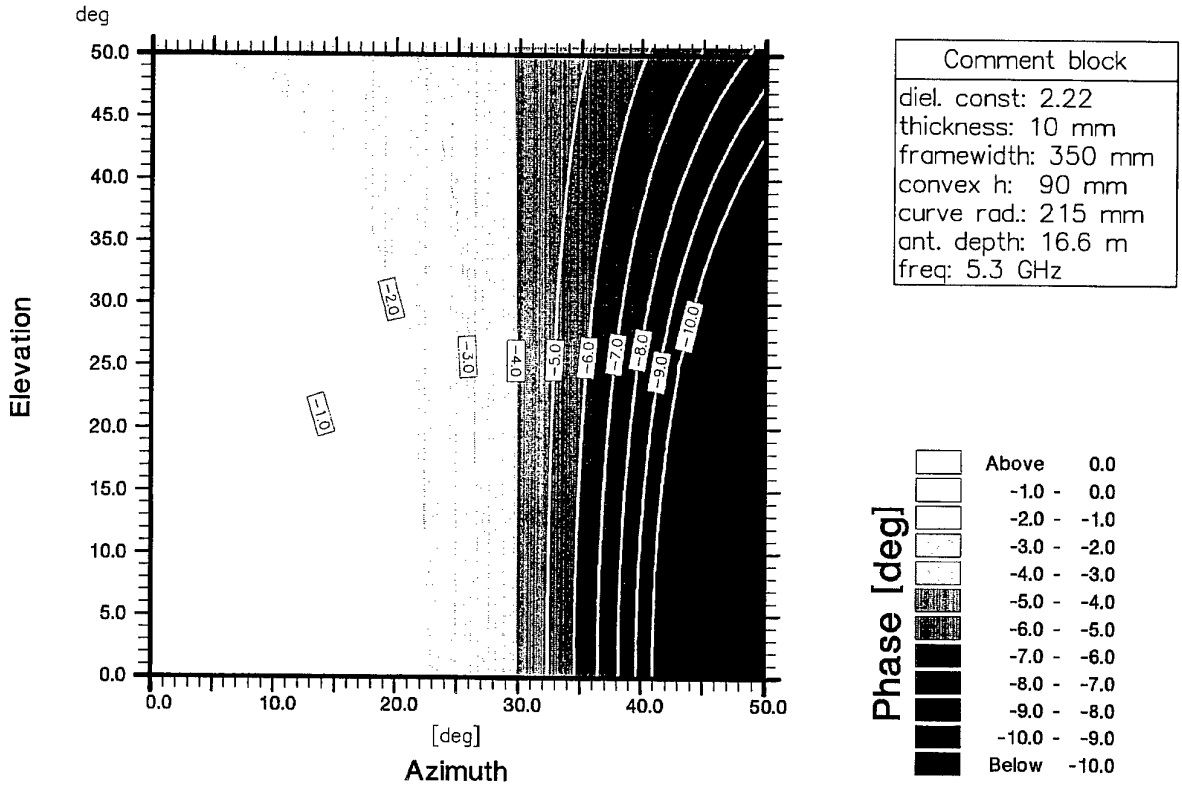

Figure A.6.a: Additional phase shift a radome of 10 mm thickness, max. height

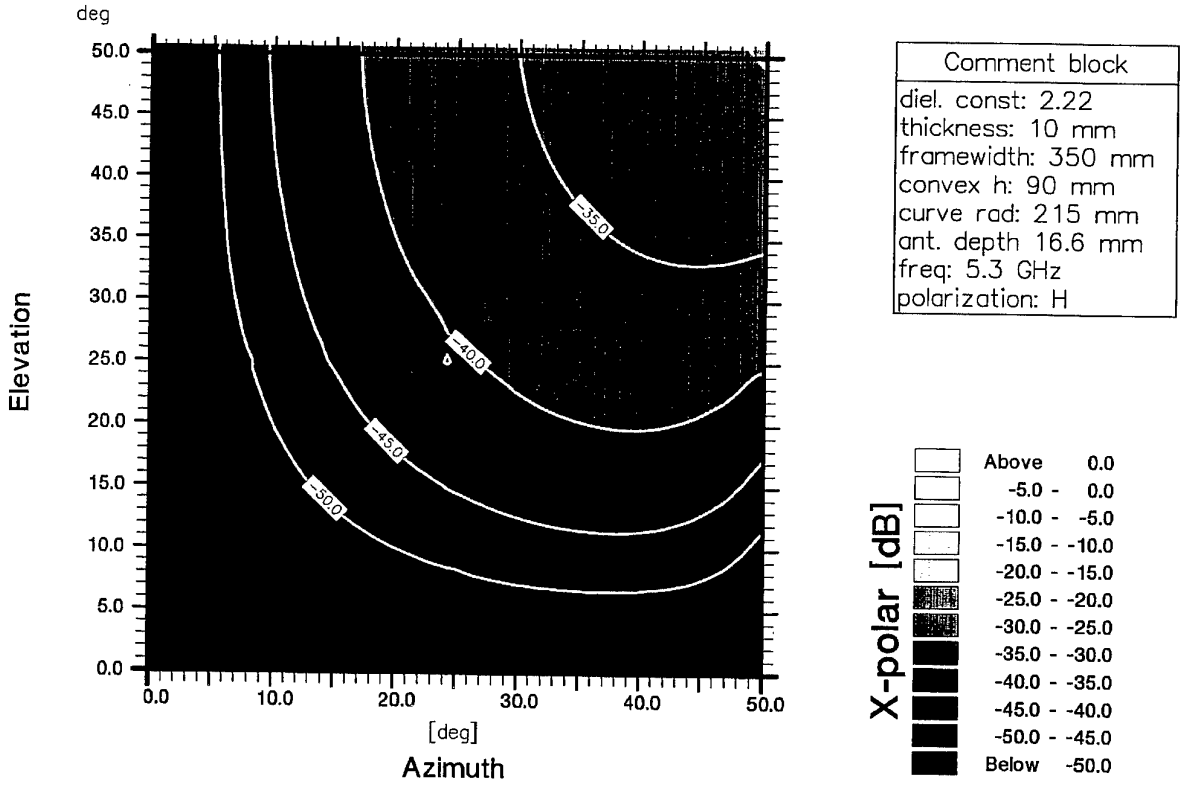

Figure A.6.b: Additional cross-polarisation of a radome of 10 mm thickness, max. heigth (the cross-polarisation performance is identical for both horizontal and vertical polarisation)

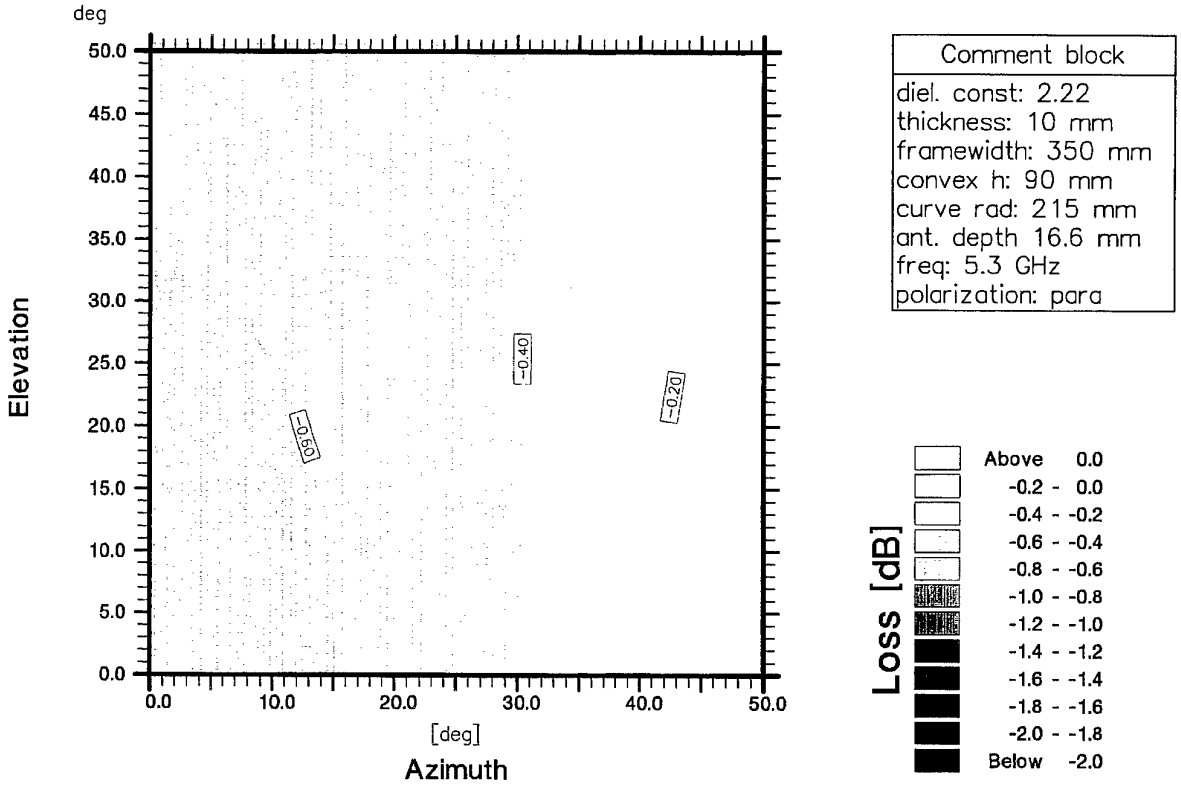

Figure A.6.c: Return loss of a radome of 10 mm thickness, max. height, parallel components

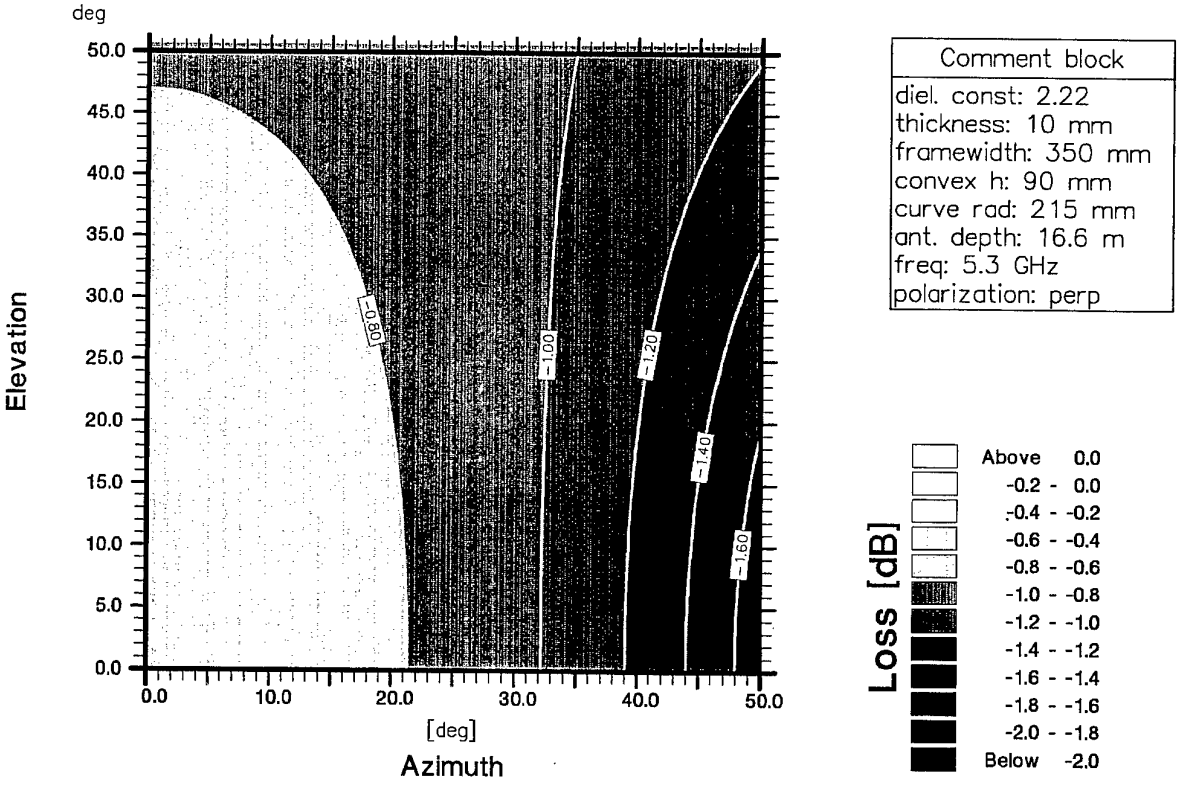

Figure A.6.d: Return loss of a radome of 10 mm thickness, max. height, perpendicular components

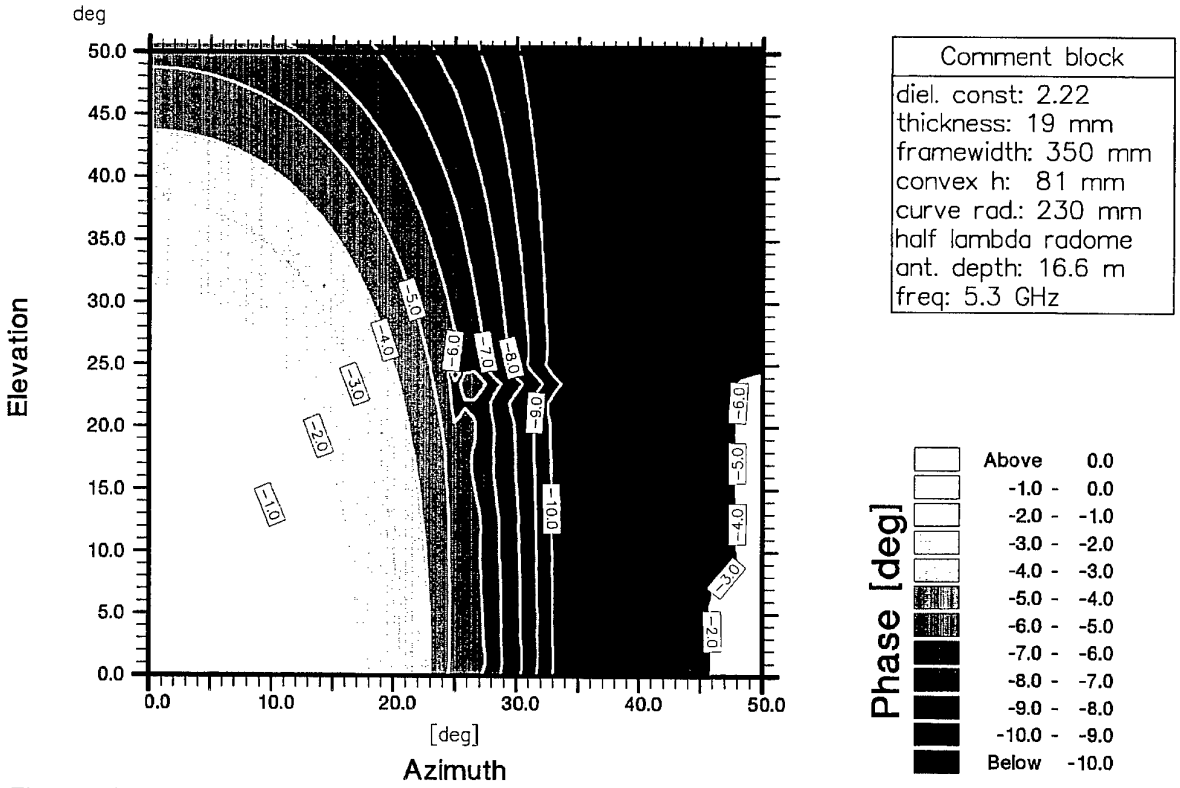

Figure A.7.a: Additional phase shift a radome of 19 mm thickness (half lambda), max. height

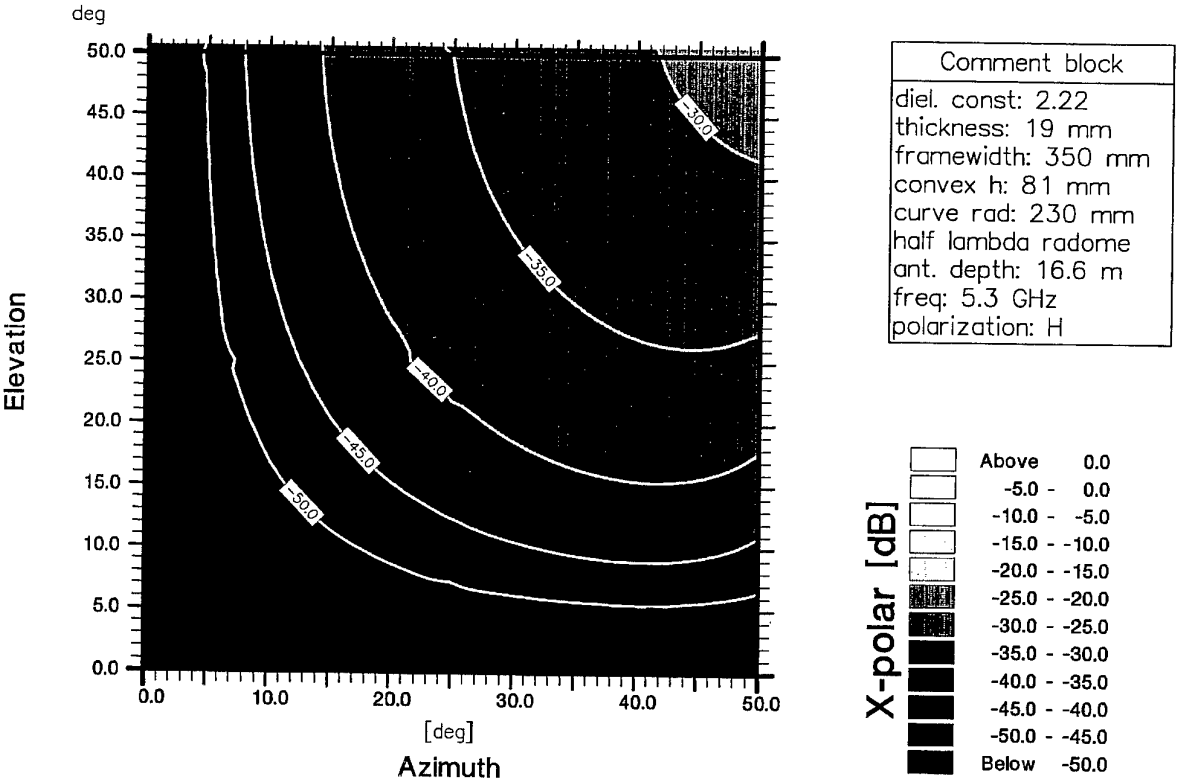

Figure A.7.b: Additional cross-polarisation of a radome of 19 mm thickness (half lambda), max. height (the cross-polarisation performance is identical for both horizontal and vertical polarisation)

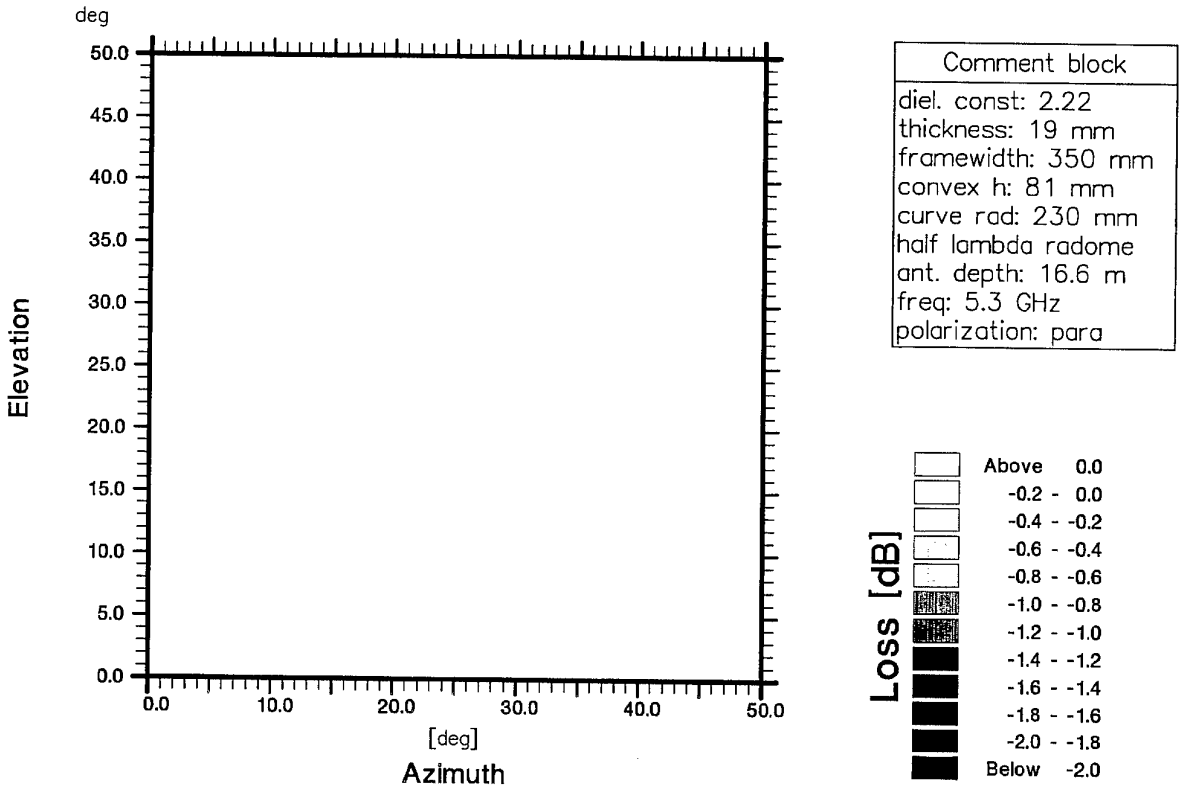

Figure A.7.c: Return loss of a radome of 19 mm thickness (half lambda), max. height, parallel components

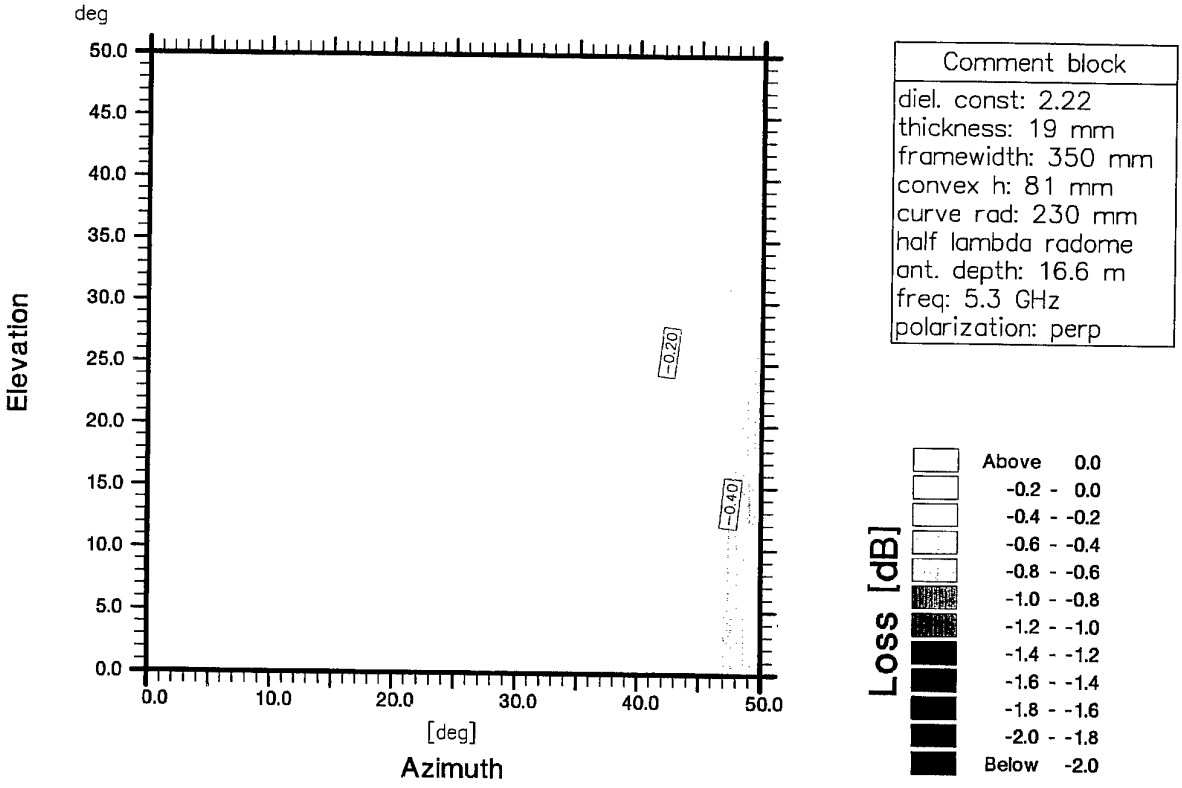

Figure A.7.d: Return loss of a radome of 19 mm thickness (half lambda), max. height, perpendicular components

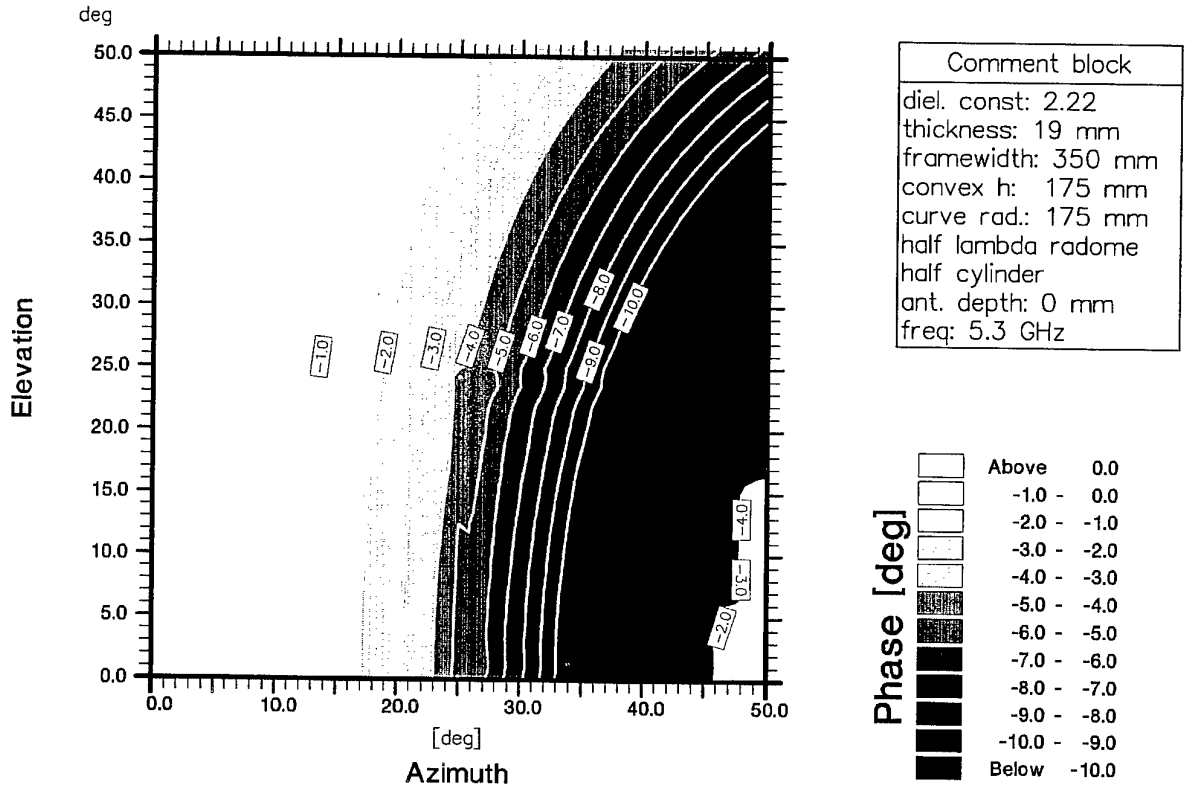

Figure A.8.a: Additional phase shift a half cylinder radome of 19 mm thickness (half lambda)

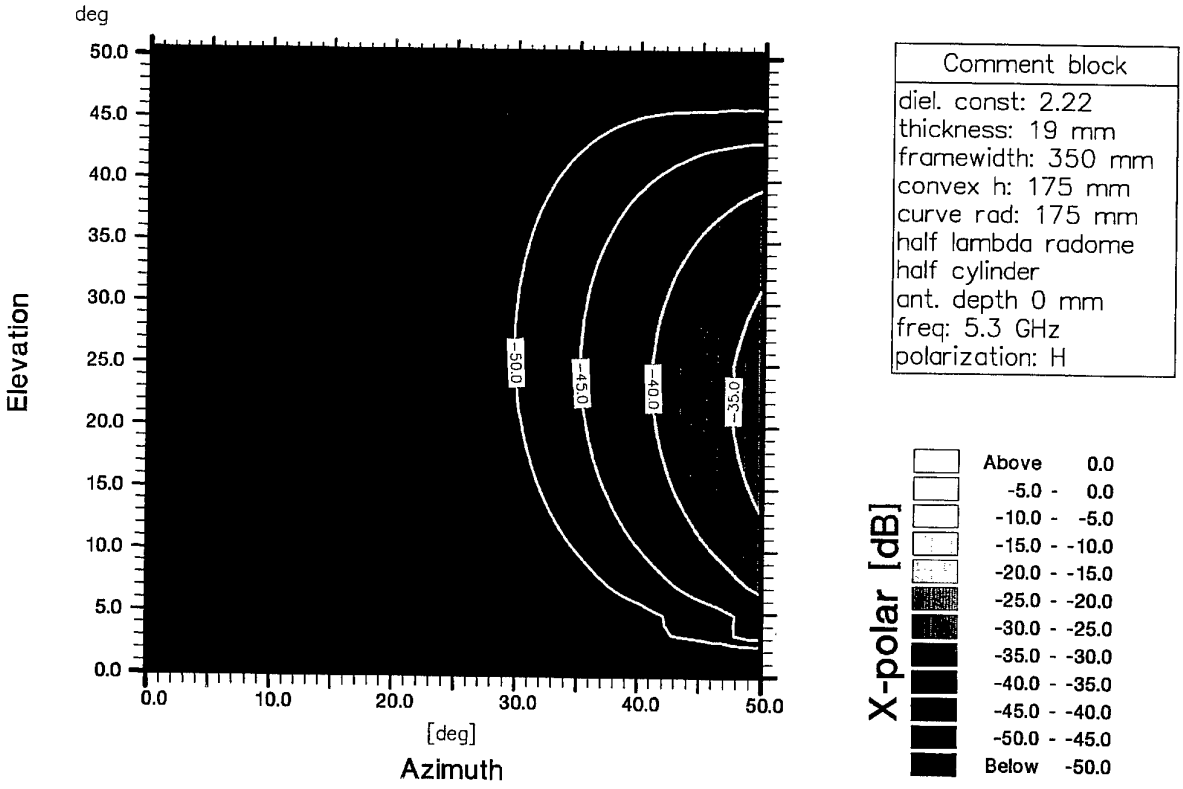

Figure A.8.b: Additional cross-polarisation of a half cylinder radome of 19 mm thickness (half lambda), (the cross-polarisation performance is identical for both horizontal and vertical polarisation)

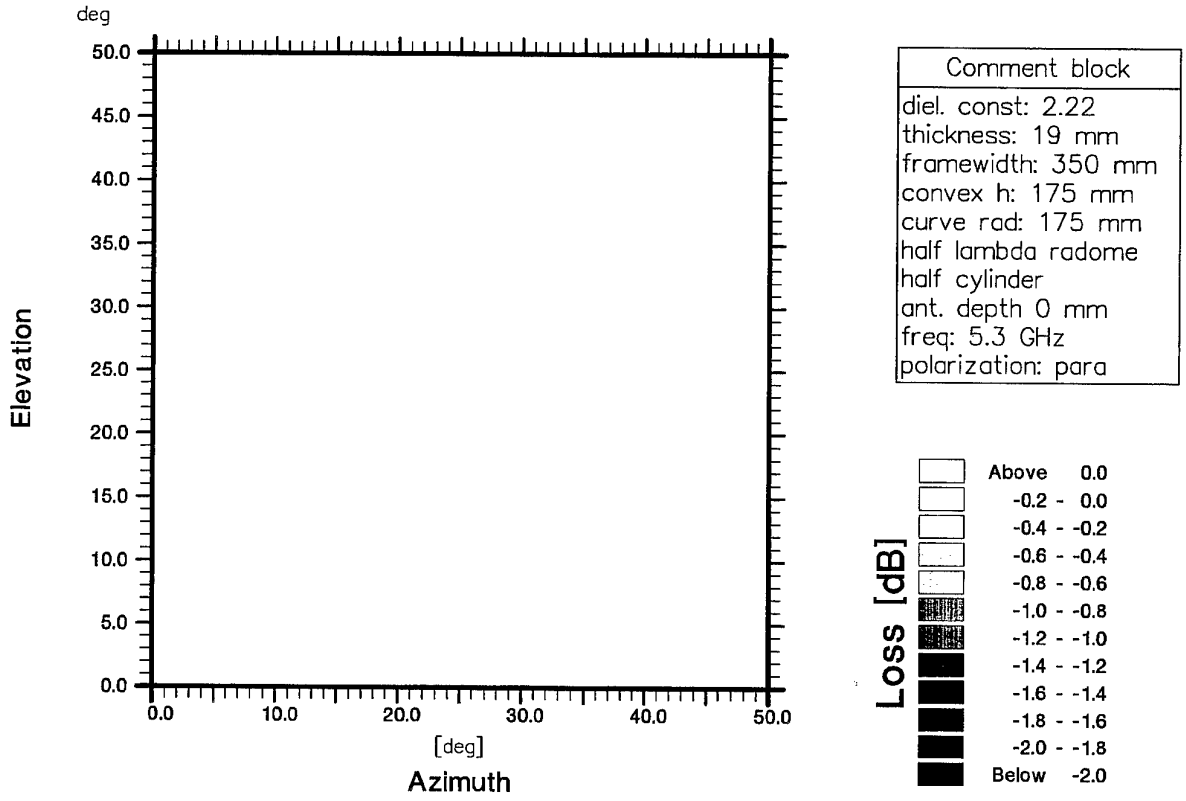

Figure A.8.c: Return loss of a half cylinder radome of 19 mm thickness (half lambda), parallel components

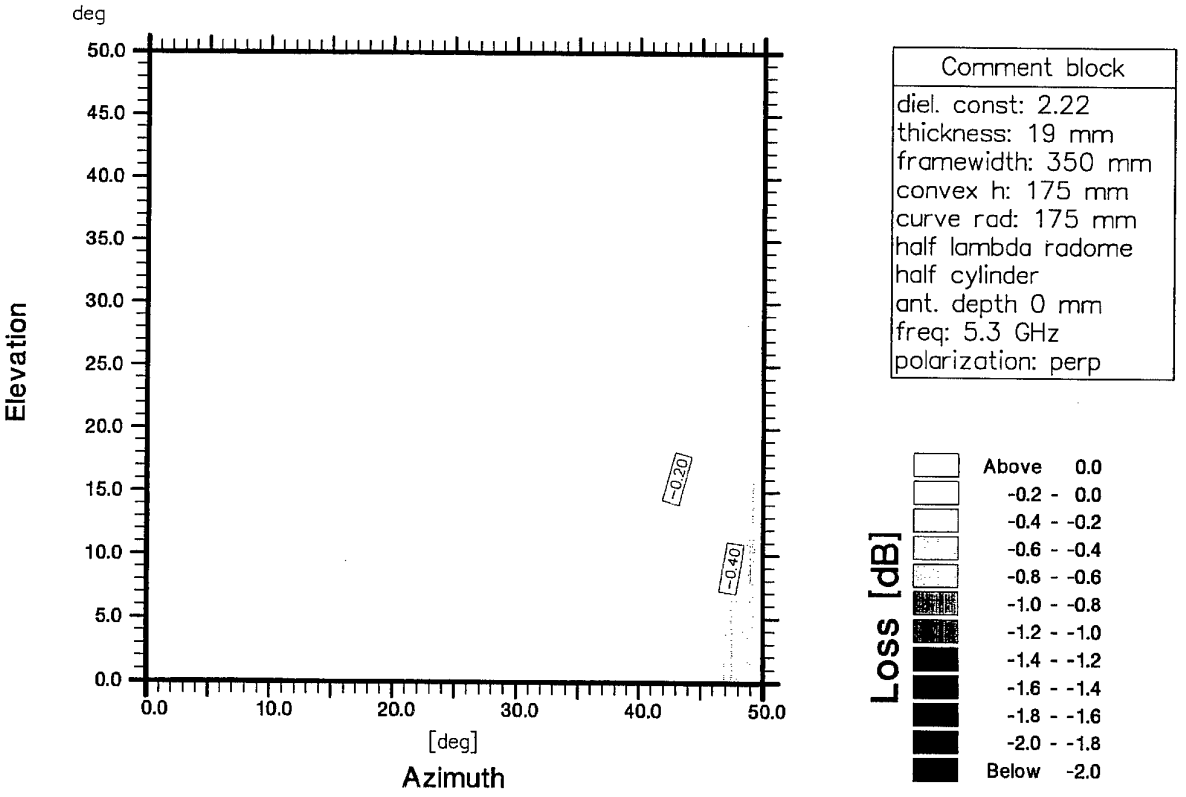

Figure A.8.d: Return loss of a half cylinder radome of 19 mm thickness (half lambda), perpendicular components

REPORT DOCUMENTATION PAGE
(MOD-NL)

1. DEFENCE REPORT NO (MOD-NL)	2. RECIPIENT'S ACCESSION NO	3. PERFORMING ORGANIZATION REPORT NO
TD96-0368		FEL-96-B216
4. PROJECT/TASK/WORK UNIT NO	**5. CONTRACT NO**	**6. REPORT DATE**
22340.8	-	November 1996
7. NUMBER OF PAGES	**8. NUMBER OF REFERENCES**	**9. TYPE OF REPORT AND DATES COVERED**
45 (incl 1 appendix, excl RDP & distribution list)	4	

10. TITLE AND SUBTITLE

Design of the PHARUS radome; Electrical aspects

11. AUTHOR(S)

M.H.A. Paquay

12. PERFORMING ORGANIZATION NAME(S) AND ADDRESS(ES)

TNO Physics and Electronics Laboratory, PO Box 96864, 2509 JG The Hague, The Netherlands
Oude Waalsdorperweg 63, The Hague, The Netherlands

13. SPONSORING AGENCY NAME(S) AND ADDRESS(ES)

TNO Physics and Electronics Laboratory, PO Box 96864, 2509 JG The Hague, The Netherlands
Oude Waalsdorperweg 63, The Hague, The Netherlands

14. SUPPLEMENTARY NOTES

The classification designation Ongerubriceerd is equivalent to Unclassified, Stg. Confidentieel is equivalent to Confidential and Stg. Geheim is equivalent to Secret.

15. ABSTRACT (MAXIMUM 200 WORDS (1044 BYTE))

Prior to the fabrication of the radome for the PHARUS-system, simulations have been made, using a method based on Single Ray Tracing and Transmission Line Equivalence. The radome, made of a Dyneema-composite, is optimized for reflection loss and the cross-polar performance. Within the mechanical restrictions, a single layer cylindrical radome with a radius of 207.5 mm and a thickness of 4 mm is the best achievable compomise. Measurements have verified that the fabricated radome is suitable for the PHARUS-system.

16. DESCRIPTORS	IDENTIFIERS
Radomes Airborne radar	

17a. SECURITY CLASSIFICATION (OF REPORT)	17b. SECURITY CLASSIFICATION (OF PAGE)	17c. SECURITY CLASSIFICATION (OF ABSTRACT)
Ongerubriceerd	Ongerubriceerd	Ongerubriceerd

18. DISTRIBUTION AVAILABILITY STATEMENT	17d. SECURITY CLASSIFICATION (OF TITLES)
Unlimited Distribution	Ongerubriceerd

Distributielijst

1.	Bureau TNO Defensieonderzoek
2.	Directeur Wetenschappelijk Onderzoek en Ontwikkeling*)
3.	HWO-KL*)
4.	HWO-KLu*)
5.	HWO-KM*)
6.	HWO-CO*)
7 t/m 9.	KMA, Bibliotheek
10.	CC-TNO
11.	NLR, t.a.v. Ir. H. Pouwels
12.	NLR, t.a.v. Ir. J.A. Hekstra
13.	Tu Delft, t.a.v. Ir. P. Snoeij
14.	DMKM/WCS, t.a.v. Ing. B. v.d. Holst
15.	DMKM/WCS, t.a.v. KLTZE J. Snoeks
16.	DMKL/Afd. ART-LUA/Sie ART/O&W, t.a.v. Ing. B.J. van Maaren
17.	DMKLu/Afd. Jachtvliegtuigen, t.a.v. Maj. Ir. L. Thoens
18.	Directie TNO-FEL, t.a.v. Dr. J.W. Maas
19.	Directie TNO-FEL, t.a.v. Ir. J.A. Vogel, daarna reserve
20.	Archief TNO-FEL, in bruikleen aan M&P, daarna reserve
21.	Archief TNO-FEL, in bruikleen aan Ir. P.J. Koomen
22.	Archief TNO-FEL, in bruikleen aan Ing. B.C.B. Vermeulen
23.	Archief TNO-FEL, in bruikleen aan Ir. H.R. van Es
24.	Archief TNO-FEL, in bruikleen aan Ir. W.P.M.N. Keizer
25.	Archief TNO-FEL, in bruikleen aan Ir. M.H.A. Paquay
26.	Archief TNO-FEL, in bruikleen aan Ir. H.J. Visser
27.	Documentatie TNO-FEL
28.	Reserve
	TNO-PML, Bibliotheek**)
	TNO-TM, Bibliotheek**)
	TNO-FEL, Bibliotheek**)

Indien binnen de krijgsmacht extra exemplaren van dit rapport worden gewenst door personen of instanties die niet op de verzendlijst voorkomen, dan dienen deze aangevraagd te worden bij het betreffende Hoofd Wetenschappelijk Onderzoek of, indien het een K-opdracht betreft, bij de Directeur Wetenschappelijk Onderzoek en Ontwikkeling.

*) Beperkt rapport (titelblad, managementuittreksel, RDP en distributielijst).
**) RDP.